Received: 4 May 2017 | Revised: 18 December 2017 | Accepted: 24 December 2017

DOI: 10.1111/gcb.14048

PRIMARY RESEARCH ARTICLE

WILEY Global Change Biology

# Soil phosphorus does not keep pace with soil carbon and nitrogen accumulation following woody encroachment

Yong Zhou | Thomas W. Boutton | X. Ben Wu

Department of Ecosystem Science and Management, Texas A&M University, College Station, TX, USA

**Correspondence**
Yong Zhou, Department of Ecosystem Science and Management, Texas A&M University, College Station, TX, USA.
Email: zhouyong1222@tamu.edu

**Funding information**
U.S. National Science Foundation, Grant/Award Number: DEB/DDIG1600790; Explorers Club; Southwestern Association of Naturalists; USDA/NIFA, Grant/Award Number: 1003961; Department of Ecosystem Science and Management at College of Agriculture and Life Science, Texas A&M University

## Abstract

Soil carbon, nitrogen, and phosphorus cycles are strongly interlinked and controlled through biological processes, and the phosphorus cycle is further controlled through geochemical processes. In dryland ecosystems, woody encroachment often modifies soil carbon, nitrogen, and phosphorus stores, although it remains unknown if these three elements change proportionally in response to this vegetation change. We evaluated proportional changes and spatial patterns of soil organic carbon (SOC), total nitrogen (TN), and total phosphorus (TP) concentrations following woody encroachment by taking spatially explicit soil cores to a depth of 1.2 m across a subtropical savanna landscape which has undergone encroachment by *Prosopis glandulosa* (an $N_2$ fixer) and other woody species during the past century in southern Texas, USA. SOC and TN were coupled with respect to increasing magnitudes and spatial patterns throughout the soil profile following woody encroachment, while TP increased slower than SOC and TN in topmost surface soils (0–5 cm) but faster in subsurface soils (15–120 cm). Spatial patterns of TP strongly resembled those of vegetation cover throughout the soil profile, but differed from those of SOC and TN, especially in subsurface soils. The encroachment of woody species dominated by $N_2$-fixing trees into this P-limited ecosystem resulted in the accumulation of proportionally less soil P compared to C and N in surface soils; however, proportionally more P accrued in deeper portions of the soil profile beneath woody patches where alkaline soil pH and high carbonate concentrations would favor precipitation of P as relatively insoluble calcium phosphates. This imbalanced relationship highlights that the relative importance of biotic vs. abiotic mechanisms controlling C and N vs. P accumulation following vegetation change may vary with depth. Our findings suggest that efforts to incorporate effects of land cover changes into coupled climate–biogeochemical models should attempt to represent C-N-P imbalances that may arise following vegetation change.

**KEYWORDS**
landscape scale, $N_2$ fixation, soil C-N-P imbalance, soil profile, spatial patterns, structural equation models, subtropical savanna, woody encroachment

## 1 | INTRODUCTION

Globally constrained ratios of carbon (C), nitrogen (N), and phosphorus (P) in marine (Redfield, 1958) and terrestrial ecosystems (Cleveland & Liptzin, 2007; McGroddy, Daufresne, & Hedin, 2004) suggest that the cycles of C, N, and P are strongly coupled by biological processes. Nevertheless, recent studies indicate that the dramatic shift in the bioavailability of essential elements resulting from anthropogenic perturbations (e.g., atmospheric deposition, N and P fertilizers, land use changes), together with continuously rising atmospheric $CO_2$ and climate changes, can provoke imbalance between C, N, and P in a variety of systems (Delgado-Baquerizo et al., 2013; Elser & Bennett, 2011; Jiao, Shi, Han, & Yuan, 2016; Peñuelas, Sardans, Rivas-ubach, & Janssens, 2012; Sistla & Schimel, 2012). As a case in point, human activities (e.g., overgrazing, fire suppression, and increased atmospheric $CO_2$, Scholes & Archer, 1997) have induced woody plant encroachment into grass-dominated dryland ecosystems. This geographically widespread vegetation change has resulted in profound effects on soil biogeochemical cycles at ecosystem to regional and global scales (Houghton, Hackler, & Lawrence, 1999; Liu, Wu, Bai, Boutton, & Archer, 2011; Pacala et al., 2001). These changes may have the potential to change the elemental balance of C, N, and P in soils, although this has not been explicitly investigated.

Plant species have unique strategies to acquire essential elements, and the supply of one element can interactively affect the cycles of others within plants or soils (Sterner & Elser, 2002). Different species generally have distinctive stoichiometries, such that changes in species composition can substantially alter the stoichiometric composition and elemental balance of an ecosystem (Elser, Fagan, Kerkhoff, Swenson, & Enquist, 2010; Sistla & Schimel, 2012). Following vegetation shift from grass to woody plant dominance, numerous studies have demonstrated net increases in soil organic C (SOC), with accumulation rates depending on climate, soil properties, and identity of encroaching woody species (Barger et al., 2011; Eldridge et al., 2011; Li et al., 2016). N and P commonly limit key ecosystem functions (e.g., primary production, Vitousek, Porder, Houlton, & Chadwick, 2010) and services (e.g., C sequestration, Hessen, Ågren, Anderson, Elser, & de Ruiter, 2004), but their supply is fulfilled in different ways. In many dryland ecosystems, woody encroachment is often facilitated by the colonization of $N_2$-fixing tree legumes (e.g., *Prosopis* in North America and *Acacia* in South Africa), which have the potential to add N to the system to overcome possible N limitation and enable rapid accumulation of C in vegetation and soils (Blaser, Shanungu, Edwards, & Olde Venterink, 2014; Boutton & Liao, 2010; Soper & Sparks, 2017). Unlike N, P is derived mainly from weathering of parent materials (Walker & Syers, 1976), and thus ecosystems begin their existence with a fixed amount of P (Vitousek et al., 2010). Since woody proliferation can result in woody patches with aboveground biomass and primary productivity orders of magnitude greater than those of grasslands they replaced (Hibbard, Schimel, Archer, Ojima, & Parton, 2003; Hughes et al., 2006), a significant amount of P may become tied up in plant biomass, potentially leading to smaller pools of soil P. However, some field studies have shown that woody encroachment actually increases total P in surface soils beneath woody patches (Blaser et al., 2014; Kantola, 2012; Sitters, Edwards, & Venterink, 2013). The underlying mechanisms remain unknown, but may be related to the deep rooting habits of encroaching woody species, enabling the transfer of deep soil P to surface soils through litterfall and root turnover (Blaser et al., 2014; Kantola, 2012). Despite dramatic influences of woody encroachment on soil C, N, and P cycles, few studies have simultaneously assessed the responses of these three elements and their accumulations at depths below the uppermost portions of the soil profile. Therefore, it remains largely unknown whether concentrations of soil C, N, and P change proportionally following woody encroachment into grasslands, especially in the largely overlooked subsurface soils.

Although soil C, N, and P cycles are strongly interlinked and controlled through biological processes (e.g., soil organic matter (SOM) input and subsequent microbial decomposition), the P cycle is further controlled through geochemical processes (e.g., dissolution and precipitation reactions; Schlesinger & Bernhardt, 2013). Woody encroachment into grasslands and subsequent changes in biotic and abiotic factors throughout the soil profile could exert different degrees of control on these biological and geochemical processes, and potentially lead to disproportionate changes in soil C, N, and P. Roots and root exudates are the primary sources of organic matter input throughout the soil profile (Rumpel & Kögel-Knabner, 2011; Schmidt et al., 2011), although aboveground litterfall contributes significantly to surface soils. Compared to herbaceous species, trees/shrubs in dryland areas typically have enlarged rhizospheres in both horizontal and vertical dimensions (Jackson et al., 1996; Schenk & Jackson, 2002), resulting in amplified SOM input throughout the soil profile following woody encroachment. Meanwhile, accumulations of soil organic C, N, and P are also determined by abiotic factors, such as physicochemical binding between SOM and soil minerals (i.e., clay and silt particles; Schmidt et al., 2011; Six, Conant, Paul, & Paustian, 2002) that affect microbial decomposition of SOM and favor the accumulation of soil C, N, and P. In addition, soil pH has been shown to affect the chemical form and solubility of inorganic P, and alkaline soils in dryland areas would generally favor the precipitation of dissolved inorganic P leached from surface soils as calcium phosphates (Carreira, Vinegla, & Lajtha, 2006; Ippolito et al., 2010; Schlesinger & Bernhardt, 2013). While there is a rich literature reporting the effects of these biotic/abiotic factors on net changes in soil C, N, and/or P following woody encroachment, individually or in combination, no studies have simultaneously tested the relative importance of these factors on all three elements. This question is especially relevant throughout the soil profile since these biotic and abiotic factors change significantly with soil depth.

Here, we assessed changes in the pool sizes and spatial patterns of SOC, TN, and TP following woody encroachment, and the relative importance of biotic and abiotic factors in influencing these changes

at the landscape scale throughout the soil profile. We hypothesized that landscape-scale accumulations of SOC, TN, and TP following woody encroachment into grasslands would be interlinked and their relative changes would be proportional throughout the soil profile. In addition, our previous studies have demonstrated that woody encroachment has dramatically increased root biomass throughout the entire soil profile (Boutton, Archer, Midwood, Zitzer, & Bol, 1998; Zhou, Boutton, & Wu, 2017) and potentially delivers more plant residues that drive the accrual of more SOC, TN, and TP compared to the grasslands being replaced. Therefore, we also hypothesized that landscape-scale accumulations of SOC, TN, and TP throughout the soil profile would be explained predominantly by root density, and, to a lesser degree, by abiotic factors, such as soil texture and pH.

## 2 | MATERIALS AND METHODS

### 2.1 | Study site

Research was conducted at the Texas A&M AgriLife La Copita Research Area (27°40′N, 98°12′W; elevation 75–90 m a.s.l.) in the eastern Rio Grande Plains, Texas, USA. The climate is subtropical (mean annual temperature 22.4°C; mean annual precipitation 680 mm). Topography at this site gently grades (1%–3% slopes) from well-drained uplands to lower lying drainage woodlands. Soils on upland portions of the landscape are sandy loams with a continuous argillic horizon (*Bt*); however, nonargillic inclusions also occur within the upland (Appendix S1; Archer, 1995; Zhou, Boutton, Wu, & Yang, 2017).

Uplands of this site were once almost exclusively dominated by $C_4$ grasses, and woody encroachment over the past century has been well documented by historical aerial photographs, tree rings, and $\delta^{13}C$ values of SOC (Archer, 1995; Archer, Scifres, Bassham, & Maggio, 1988; Bai, Boutton, Liu, Wu, & Archer, 2012; Boutton et al., 1998). Currently, upland landscapes consist of three landscape elements: grasslands, clusters (woody patches <100 $m^2$), and groves (>100 $m^2$; Appendix S1; Figure 1). The formation of clusters is initiated by the colonization of honey mesquite (*Prosopis glandulosa*; an $N_2$-fixing tree legume, Zitzer, Archer, & Boutton, 1996; Soper, Boutton, & Sparks, 2015) in grasslands. Established honey mesquite trees then serve as nurse plants and facilitate the recruitment of numerous other woody species beneath their canopy (Archer et al., 1988). If clusters occur on nonargillic inclusions, they expand and coalesce to form large groves (Appendix S1; Archer, 1995; Bai et al., 2012; Zhou, Boutton, Wu, & Yang, 2017). Groves are dominated by honey mesquite with an understory consisting of approximately 15 other subordinate woody species (Appendix S2). Although clusters are composed of the same woody species as groves, honey mesquite in clusters are usually significantly younger and smaller than those in groves (Boutton et al., 1998; Liu, Wu, Bai, Boutton, & Archer, 2010), and some were already dead (Archer, 1995; Zhou, Boutton, Wu, & Yang, 2017). The remnant grassland matrix is not only dominated by $C_4$ grasses but also includes a significant proportion of forbs ($C_3$ plants) and a smaller proportion of cacti (crassulacean acid metabolism or CAM plants). Species composition within our upland landscape study area is provided in Appendix S2.

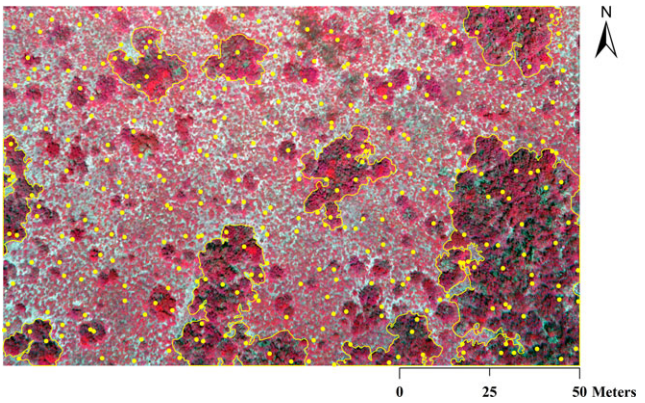


**FIGURE 1** Color-infrared aerial view of this 160 m ×100 m landscape showing locations of 320 random soil samples (yellow points). Red areas are woody clusters and groves, and light gray areas indicate open grasslands. Groves are highlighted with yellow lines. Modified from Zhou, Boutton, and Wu (2017) [Colour figure can be viewed at wileyonlinelibrary.com]

### 2.2 | Field sampling

In order to quantify patterns of spatial heterogeneity in soil C, N, and P that have been altered by woody plant encroachment, a 160 × 100 m upland landscape which included all three landscape elements (i.e., grasslands, clusters, and groves) was established and subdivided into 10 × 10 m grid cells in January 2002 (Figure 1; Liu et al., 2011). The X, Y coordinates of the corners of each grid cell were determined using a GPS unit based on UTM coordinates system (14 North, WGS 1984). A color-infrared aerial photograph of this landscape was acquired in July 2015. Edges of woody patches (clusters and groves) were manually delineated in the aerial photo using ArcGIS 10.1 (ESRI, Redlands, CA, USA) in order to create a classified vegetation map.

In July 2014, two sample points were selected randomly within each 10 × 10 m grid cell (320 points in total; Figure 1). The landscape element present at each sample point was classified as grassland ($n$ = 200), cluster ($n$ = 41), or grove ($n$ = 79) based on woody canopy area and vegetation type. The distances from each sample point to two georeferenced grid cell corners were recorded. At each sample point, two adjacent soil cores (2.8 cm in diameter and 120 cm in length) were collected using the PN150 JMC Environmentalist's Subsoil Probe (Clements Associates Inc., Newton, IA, USA). This random sampling scheme, stratified within the systematic 10 × 10 m grid cells, has been shown to effectively capture the overall spatial pattern of SOC on this landscape comprised of multiple vegetation elements (Liu et al., 2011).

### 2.3 | Lab analyses

Each soil core was subdivided into six depth increments (i.e., 0–5, 5–15, 15–30, 30–50, 50–80, and 80–120 cm). The depth increments

between 0 and 30 cm span the A-horizon, while increments between 30 and 120 cm span the B-horizon (Boutton et al., 1998). One soil core was used to estimate fine (<2 mm in diameter) and coarse (>2 mm in diameter) root biomass by washing through sieves. No attempt was made to distinguish between live or dead roots. Retrieved roots were washed carefully to remove soil particles, and dried (65°C for 48 hr) for biomass determination.

The other soil core was air-dried and then passed through a 2 mm sieve to remove coarse organic fragments. An aliquot of sieved soils was used to determine soil pH on a 1: 2 (10 g soil: 20 ml, 0.01 mol/L $CaCl_2$) mixture using a glass electrode, and soil texture by the hydrometer method (Sheldrick & Wang, 1993). A separate soil aliquot was dried at 65°C for 48 hr, pulverized in a centrifugal mill, and used for analyses of SOC, TN, and TP. Soil TN was quantified by combustion/gas chromatography using a Costech ECS 4010 elemental analyzer (Costech Analytical Technologies Inc., Valencia, CA, USA). Soil organic C concentrations were determined using the same method, but soils were pretreated with HCl vapor in a desiccator for 8 hr to remove carbonates (Harris, Horwáth, & van Kessel, 2001), and then dried. Soil TP was extracted using the lithium fusion method (Lajtha, Driscoll, Jarrell, & Elliott, 1999), and P concentrations in extracted solutions were determined by the molybdenum blue colorimetry method (Murphy & Riley, 1962) using a Spectronic $20D^+$ spectrophotometer (Thermo Fisher Scientific, Inc., Waltham, MA, USA).

Leaf and fine root tissues of each major species occurring on this landscape were collected in September 2016 (Appendix S2). Fine root tissues were collected by soil excavation that unequivocally confirmed linkages to identified plant species. These tissues were washed carefully, dried, and pulverized. Plant tissue C and N concentrations were determined by combustion/gas chromatography, and P concentrations by lithium fusion, as described above.

## 2.4 | Data analyses

Variable means of SOC, TN, and TP within each depth increment for soil cores from different landscape elements were compared using mixed models in JMP pro 12.0 (SAS Institute Inc., Cary, NC, USA). In mixed models, spatial autocorrelation of each variable was considered as a spatial covariance for adjustment (Littell, Stroup, Milliken, Wolfinger, & Schabenberger, 2006). An alpha level of 0.05 was used to determine statistical significance. Variogram analyses were performed to quantify the spatial structures of SOC, TN, and TP for each depth increment based on 320 random samples across this landscape using the "gstat" package in R statistical software (R Development Core Team 2014). Ordinary kriging was used for spatial interpolation based on parameters obtained from variogram analyses (Appendix S3), and kriged maps of SOC, TN, and TP within each depth increment were generated using ArcMap 10.1 (ESRI, Redlands, CA, USA).

A scaling approach was used to test the proportional changes between SOC, TN, and TP following woody encroachment into grasslands. We plotted $\log_{10}$-transformed soil TN or TP (mg N or P $kg^{-1}$ soil) on the *y*-axis and $\log_{10}$-transformed SOC (mg C $kg^{-1}$ soil) on the *x*-axis to test whether soil TN and TP changed systematically with SOC accumulation (Appendix S4). If soil TN and TP accumulate in proportion to accrual of SOC, we would expect that slopes of the N-C and P-C stoichiometric relationships would not be significantly different from 1.0 (i.e., the 95% confidence intervals of the scaling slope included 1.0; Appendix S4). If there were directional increases in proportion of soil TN and TP with increasing SOC, we would expect scaling slopes greater than 1.0; in contrast, if there were directional decreases in the proportion of soil TN and TP with increasing SOC, we would expect scaling slopes <1.0 (Appendix S4). Scaling slopes of N-C and P-C stoichiometric relationships were determined by reduced major axis regression (i.e., type II regression; Cleveland & Liptzin, 2007; McGroddy et al., 2004; Niklas & Cobb, 2005; Reich, Walters, & Ellsworth, 1997; Yang & Luo, 2011) using the "lmodel2" package in R statistical software.

To assess the relative importance of fine roots and soil physicochemical properties on accumulations of SOC, TN, and TP within each depth increment throughout the soil profile, we used structural equation models (SEM), which are based on a priori information regarding the relationships among the explanatory and response variables of interest. Compared to other statistical analyses, such as multiple regressions, SEM can assign directions to several relationships resulting in multiple explanatory as well as multiple response variables in a single model (Grace, 2006). Based on current ecological knowledge, we constructed our conceptual a priori SEM (Figure 2). In our conceptual model, we chose soil clay and silt content to be the only exogenous variable as spatial heterogeneity of subsurface soil texture is an intrinsic feature of this landscape (Archer, 1995; Zhou, Boutton, Wu, & Yang, 2017). By regulating the distribution of

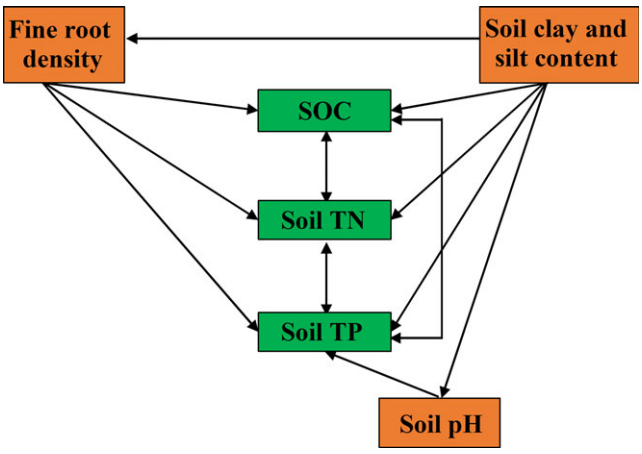


**FIGURE 2** A priori conceptual structural equation model depicting pathways by which fine root density, soil clay and silt content, and soil pH may influence the accumulation of soil organic carbon (SOC), total nitrogen (TN), and total phosphorus (TP) throughout the soil profile following woody encroachment. Single-headed arrows represent hypothesized causal relationships of one variable upon the other. Double-headed arrows signify correlations between two variables, but no direction is specified [Colour figure can be viewed at wileyonlinelibrary.com]

grove vegetation which occurs on nonargillic inclusions (Zhou, Boutton, Wu, & Yang, 2017), soil clay and silt content could affect the size and depth distribution of fine roots (Figure 2). We accounted for the fact that roots are the primary sources of organic matter input in soil by including them in our conceptual model (Figure 2). We also related soil clay and silt content to SOC, TN, and TP because it has been shown that intimate associations between organic matter and fine soil particles (i.e., clay and silt) is an important mechanism for the accumulation/stabilization of organic matter in soils (Figure 2). Soil pH was linked with soil TP because the fixation of soluble P with soil minerals to form insoluble compounds is affected by soil pH (Figure 2). Descriptive statistics (i.e., mean and standard error) for fine root density, soil texture, and soil pH can be found in Zhou, Boutton, and Wu (2017). Meanwhile, our conceptual model included correlations between SOC, TN, and TP in order to detect changes in their stoichiometric relationships throughout the soil profile.

To evaluate the fit of the SEM models, we used $\chi^2$ goodness-of-fit test and the root mean squared error of approximation (RMSEA) according to Grace (2006). The $\chi^2$ test assesses the magnitude of difference between the observed and expected covariance matrix of the SEM. Therefore, if the value of $\chi^2$ is close to zero, it indicates small differences and thus a good fit. RMSEA assesses the magnitude of the approximation error per degree of freedom, and a value of RMSEA close to zero indicates a good fit (Grace, 2006). In order to facilitate comparisons between different depth increments, we did not simplify our a priori model by excluding nonsignificant paths. Dataset were $\log_{10}$-transformed to improve the normality prior to constructing SEMs using AMOS 24.0 (Amos Development Co., Armonk, NY, USA).

## 3 | RESULTS

### 3.1 | Stoichiometric composition of different plant life-forms

Overall, leaves had higher mean C, N, and P concentrations than fine roots (Figure 3). Although not all significant, woody species (both

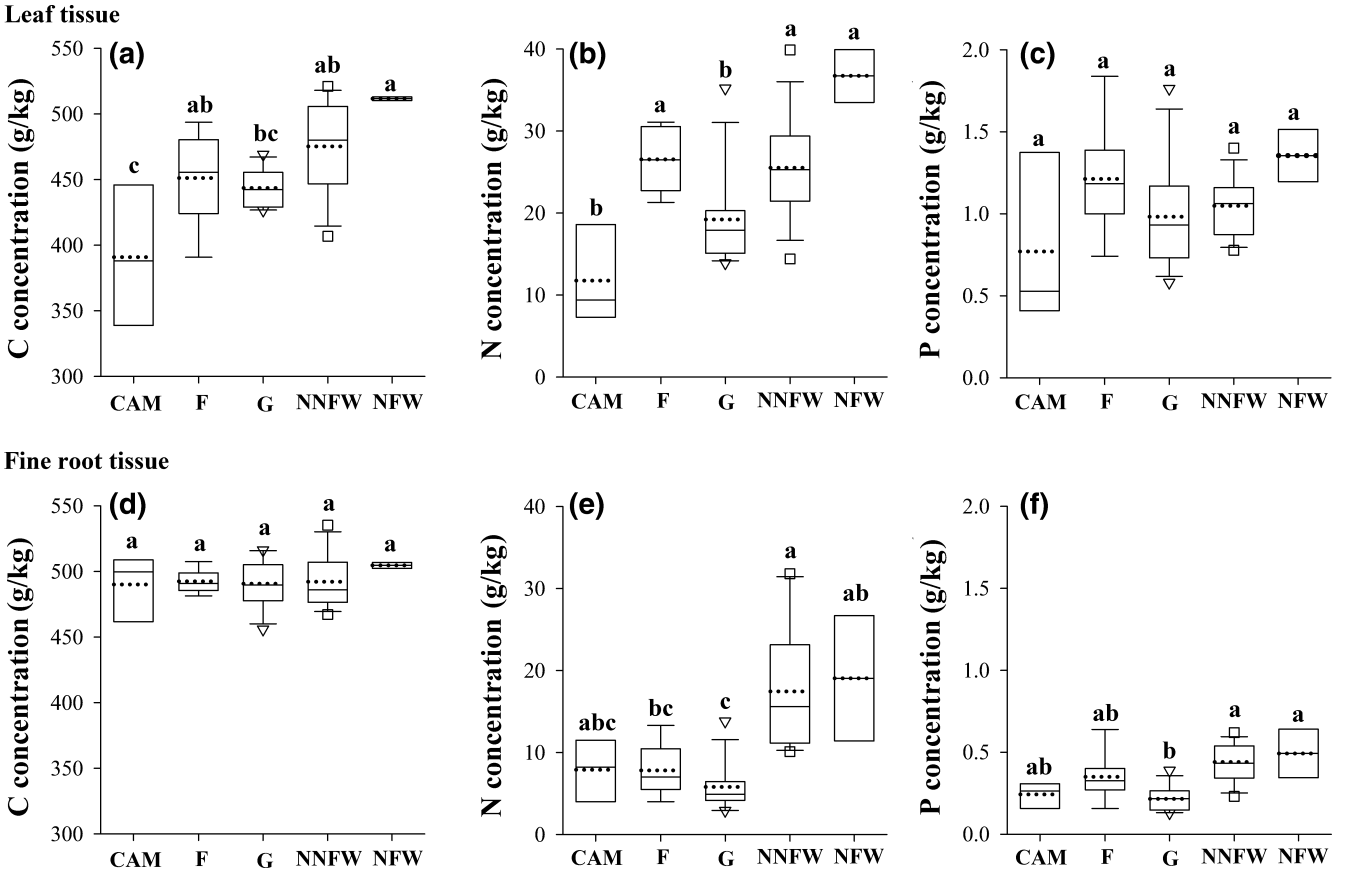


**FIGURE 3** Carbon (C), nitrogen (N), and phosphorus (P) concentrations (g/kg) of leaf and fine root tissues for different plant life-forms occurring on this landscape. The box plots summarize the distribution of points for each variable within each plant life-form. The central box shows the interquartile range, median (horizontal solid line in the box), and mean (horizontal dotted line in the box). Lower and upper error bars indicate 10th and 90th percentiles, and points above and below the error bars (boxes and triangles) are individuals below the 10th or above the 90th percentiles. Statistical significance is based on Tukey tests and indicated with different letters. CAM, crassulacean acid metabolism species, $n = 3$; F, forbs, $n = 9$; G, grasses, $n = 13$; NNFW, non–$N_2$-fixing woody species, $n = 13$; NFW, $N_2$-fixing woody species, $n = 2$. For more details, see Appendix S2

non-$N_2$ fixers and $N_2$ fixers) had higher mean C, N, and P concentrations than grasses in both leaf and fine root tissues (Figure 3). $N_2$-fixing woody species had highest mean C, N, and P concentrations in both leaves and fine roots (Figure 3). In addition, it is worth noting that N concentrations in leaf and fine root tissues of $N_2$-fixing woody species were 1.9 and 3.3 times higher, respectively, than those of grasses; in contrast, P concentrations in leaves and fine roots were only 1.4 and 2.3 times higher in $N_2$-fixing woody plants vs. grasses, respectively (Figure 3).

## 3.2 | Imbalanced soil P with respect to C and N throughout the soil profile

Overall, woody encroachment into grassland increased SOC, TN, and TP concentrations across this landscape and throughout the entire 120 cm soil profile, albeit in different magnitudes (Table 1). SOC and TN were strongly coupled as their proportional increases following woody encroachment were similar within each soil depth increment (Table 1). This strong coupled relationship is validated by multiple lines of evidence. Firstly, strong positive correlations between soil P: N vs. P: C ratios throughout the soil profile were observed (Figure 4). Secondly, slopes for N-C stoichiometric relationship throughout the soil profiles were consistently near 1.0 across this landscape (Table 2) and slopes for clusters and groves were much similar to those for grasslands (Table 2). Thirdly, spatial patterns of SOC and TN were identical to each other for each depth increment (Figure 5). Last but not least, SOC and TN were highly correlated with each other ($r > .80$) as shown in SEMs (Figure 6).

However, TP was uncoupled from SOC and TN, especially for grove vegetation which is the dominant feature creating spatial heterogeneity in this landscape. In the 0–5 cm depth increment, the percentage increases in SOC and TN were 2.5 times greater than for TP under groves compared to grasslands (Table 1). This proportionally smaller increase in soil TP has resulted in (1) soil samples from groves were scattered below those of grasslands in the plots of soil N: C vs. P: C ratios (Figure 4; Appendix S5); and (2) slopes of the P-C stoichiometric relationship for groves in the 0–5 cm depth increment were much <1.0 (Table 2). In the 5–15 cm depth increment, the percentage increase in soil TP under groves was comparable to that of SOC and TN (Table 1), thus, the slope of the P-C stoichiometric relationship for groves was not different from 1.0 (Table 2). In contrast, percentage increases in TP under groves in the 15–30, 30–50, and 50–80 cm depth increments were several to more than 10 times higher than those of SOC and TN at those same depths

**TABLE 1** Mean and standard error (*SE*) of soil organic carbon (SOC) (a), total nitrogen (TN) (b), and total phosphorus (TP) (c) in contrasting landscape elements, and also percentage increases in those values from grassland to cluster or grove throughout the soil profile in a subtropical savanna

| | Landscape element | | | | | | Percentage increases | |
|---|---|---|---|---|---|---|---|---|
| | Grassland | | Cluster | | Grove | | | |
| Depth (cm) | Mean | *SE* | Mean | *SE* | Mean | *SE* | Grassland to Cluster | Grassland to Grove |
| (a) SOC (g C $kg^{-1}$ soil) | | | | | | | | |
| 0–5 | $6.68^c$ | 0.12 | $16.95^b$ | 1.44 | $22.14^a$ | 1.36 | 153.7 | 231.4 |
| 5–15 | $5.44^b$ | 0.05 | $8.23^a$ | 0.45 | $8.78^a$ | 0.26 | 51.3 | 61.4 |
| 15–30 | $5.11^b$ | 0.04 | $6.02^a$ | 0.16 | $6.29^a$ | 0.12 | 17.8 | 23.1 |
| 30–50 | $4.96^a$ | 0.05 | $5.32^a$ | 0.11 | $5.34^a$ | 0.12 | 7.3 | 7.7 |
| 50–80 | $3.51^b$ | 0.03 | $3.93^a$ | 0.09 | $3.86^a$ | 0.07 | 12.0 | 10.0 |
| 80–120 | $2.28^b$ | 0.03 | $2.61^a$ | 0.10 | $2.90^a$ | 0.06 | 14.5 | 27.2 |
| (b) Soil TN (g N $kg^{-1}$ soil) | | | | | | | | |
| 0–5 | $0.65^c$ | 0.01 | $1.57^b$ | 0.12 | $2.09^a$ | 0.12 | 141.5 | 221.5 |
| 5–15 | $0.56^b$ | 0.01 | $0.83^a$ | 0.04 | $0.88^a$ | 0.02 | 48.2 | 57.1 |
| 15–30 | $0.51^a$ | 0.00 | $0.59^a$ | 0.02 | $0.62^a$ | 0.01 | 15.7 | 21.6 |
| 30–50 | $0.52^a$ | 0.01 | $0.54^a$ | 0.01 | $0.53^a$ | 0.01 | 3.8 | 1.9 |
| 50–80 | $0.41^b$ | 0.00 | $0.44^a$ | 0.01 | $0.42^a$ | 0.01 | 7.3 | 2.4 |
| 80–120 | $0.28^b$ | 0.00 | $0.31^a$ | 0.01 | $0.34^a$ | 0.01 | 10.7 | 21.4 |
| (c) Soil TP (mg P $kg^{-1}$ soil) | | | | | | | | |
| 0–5 | $81.7^c$ | 0.7 | $124.0^b$ | 3.9 | $154.2^a$ | 4.3 | 51.8 | 88.7 |
| 5–15 | $76.5^c$ | 0.6 | $95.3^b$ | 2.3 | $123.7^a$ | 3.6 | 24.6 | 61.7 |
| 15–30 | $75.9^c$ | 0.6 | $85.0^b$ | 1.8 | $119.1^a$ | 3.4 | 12.0 | 56.9 |
| 30–50 | $84.8^b$ | 0.7 | $89.0^b$ | 1.7 | $123.2^a$ | 3.1 | 5.0 | 45.3 |
| 50–80 | $80.0^c$ | 0.6 | $87.8^b$ | 1.5 | $112.5^a$ | 2.8 | 9.8 | 40.6 |
| 80–120 | $71.0^c$ | 0.5 | $77.4^b$ | 1.6 | $99.3^a$ | 2.1 | 9.0 | 39.9 |

Significant differences between means in landscape elements are indicated with different superscript letters. Number of samples: grassland = 200, cluster = 41, and grove = 79. Please note that units for soil TP (mg P $kg^{-1}$ soil) are different than those for SOC (g C $kg^{-1}$ soil) and soil TN (g N $kg^{-1}$ soil).

(Table 1). Correspondingly, (1) soil samples from groves were scattered above those of grasslands in these depth increments (Figure 4; Appendix S5); and (2) slopes for groves were >1.0 in these depth increments (Table 2). The percentage increases in soil TP under clusters were less than those for SOC and TN in the 0–5, 5–15, 50–80, and 80–120 cm depth increments, but comparable in the 15–30 and 30–50 cm depth increments (Table 1 and Table 2). Due to the substantial increase in TP under groves throughout the soil profiles (Table 1), spatial patterns of soil TP for every depth increment displayed strong resemblance to that of vegetation cover (Figure 5). Spatial patterns of TP were distinctive from those of SOC and TN, especially in subsurface soils (>15 cm; Figure 5). These decoupled responses of soil TP from those of SOC and TN throughout the soil profile resulted in correlations between soil P : C and N : C ratios and between SOC and TN that were not strong, especially for these intermediate depth increments (Figures 4 and 6).

### 3.3 | Factors influencing imbalanced accumulation change throughout the soil profile

Goodness-of-fit tests for SEMs indicated that the data from the 0–5, 15–30, 30–50, and 50–80 cm depth increments fitted the a priori model well, as both $\chi^2$ and RMSEA were close to zero (Figure 6). Thus, our SEMs can be accepted as potential explanations for the observed variance in SOC, TN, and TP throughout the soil profile. Overall, the powers of explanation for the variance in SOC, TN, and TP decreased with soil depth (Figure 6). For example, in the 0–5 cm depth increment, the model explained 63%, 65%, 63% of the variance in SOC, TN, and TP, respectively, whereas these values were 26%, 25%, 38% in the 80–120 cm depth increment (Figure 5). Fine root density, soil clay and silt content, and soil pH showed positive relationships with SOC, TN, and TP throughout the soil profile (Figure 6).

The effects of fine root density, soil clay and silt content, and soil pH on SOC, TN, and TP changed with soil depth (Figure 7). For example, in the 0–5 cm depth increment, fine root density, as a biotic factor, explained the greatest proportion of the variance in SOC, TN, and TP, with minor contributions from soil clay and silt content (Figure 7). However, the relative importance of fine root density decreased throughout the soil profile; instead, soil clay and silt content explained a significant proportion of the variance in SOC and TN, while soil pH accounted for an important portion of the variance in soil TP (Figure 7). This is especially true for the 30–50 cm depth increment where clay and carbonate C start to accumulate.

## 4 | DISCUSSION

Our findings showed that concentrations of SOC, TN, and TP increased following woody encroachment into grasslands in this subtropical savanna, consistent with other studies around the world (Barger et al., 2011; Blaser et al., 2014; Chiti et al., 2017; Eldridge et al., 2011; Kantola, 2012; Maestre et al., 2009; Sitters et al., 2013). Contrary to our first hypothesis that landscape-scale accumulation of SOC, TN, and TP would be interlinked and their relative changes would be proportional throughout the soil profile following woody encroachment, only SOC and TN were interlinked throughout the soil profile, with both increasing in similar proportions and yielding comparable spatial patterns following woody encroachment. Soil TP was uncoupled from SOC and TN, increasing more slowly than SOC and TN in surface soils (0–5 cm, hereafter) but faster in subsurface soils (15–120 cm, hereafter). This imbalanced soil C-N-P relationship was likely a consequence of changes in the relative importance of biotic and abiotic factors throughout the soil profile. Since abiotic factors, such as soil clay and silt content and soil pH, were much more important than biotic factors (i.e., fine root density) in explaining variation in SOC, TN, and TP in subsurface soils, we also reject our second hypothesis that landscape-scale accumulations of SOC, TN, and TP throughout the soil profile would be explained predominantly by root density.

### 4.1 | Soil C-N-P imbalance in surface soils following woody encroachment

Woody proliferation is often accompanied by significant increases in primary productivity (Barger et al., 2011; Hibbard et al., 2003; Hughes et al., 2006), and rapidly growing trees/shrubs require the coupled use of N and P resources to meet the high demands for C accumulation (Sterner & Elser, 2002). In this subtropical savanna, woody encroachment is facilitated by the colonization of $N_2$-fixing honey mesquite trees, which drives N accumulation in this system (Boutton & Liao, 2010; Soper & Sparks, 2017). Nitrogen concentrations in leaf and root tissues of honey mesquite trees were two times and five times greater, respectively, than those of grass leaves and fine roots (Figure 3, Appendix S2). This additional N may trigger a positive feedback through a combination of less conservative N-use efficiency, increased deposition of N-rich litter, and faster microbial N-mineralization, thereby creating an N-enriched soil environment that may benefit other woody species under or near honey mesquite trees (Bai et al., 2008; McCulley, Archer, Boutton, Hons, & Zuberer, 2004; Soper & Sparks, 2017).

Results from the scaling approach showed that the slopes of P-C stoichiometric relationships for grasslands were consistent smaller than 1 (Table 2). This indicates that, prior to woody plant encroachment, grassland soils contained disproportionately less P than C, and are potentially P limited. Despite this, encroaching woody plant species across this landscape had higher P concentrations in leaf and fine root tissues than grasses, especially in fine root tissues of $N_2$-fixing woody species (Figure 3, Appendix S2), indicating that they have strategies to overcome P limitation. For example, woody species have more extensive and intensive root systems compared to grasses, especially in the vertical dimension (Jackson et al., 1996; Schenk & Jackson, 2002), enabling them to mine P (i.e., deep acquisition) located below the depth of grass root systems (Blaser et al., 2014; Kantola, 2012; Scholes & Archer, 1997; Sitters et al., 2013). In addition, $N_2$-fixing woody species generally maintain a high root

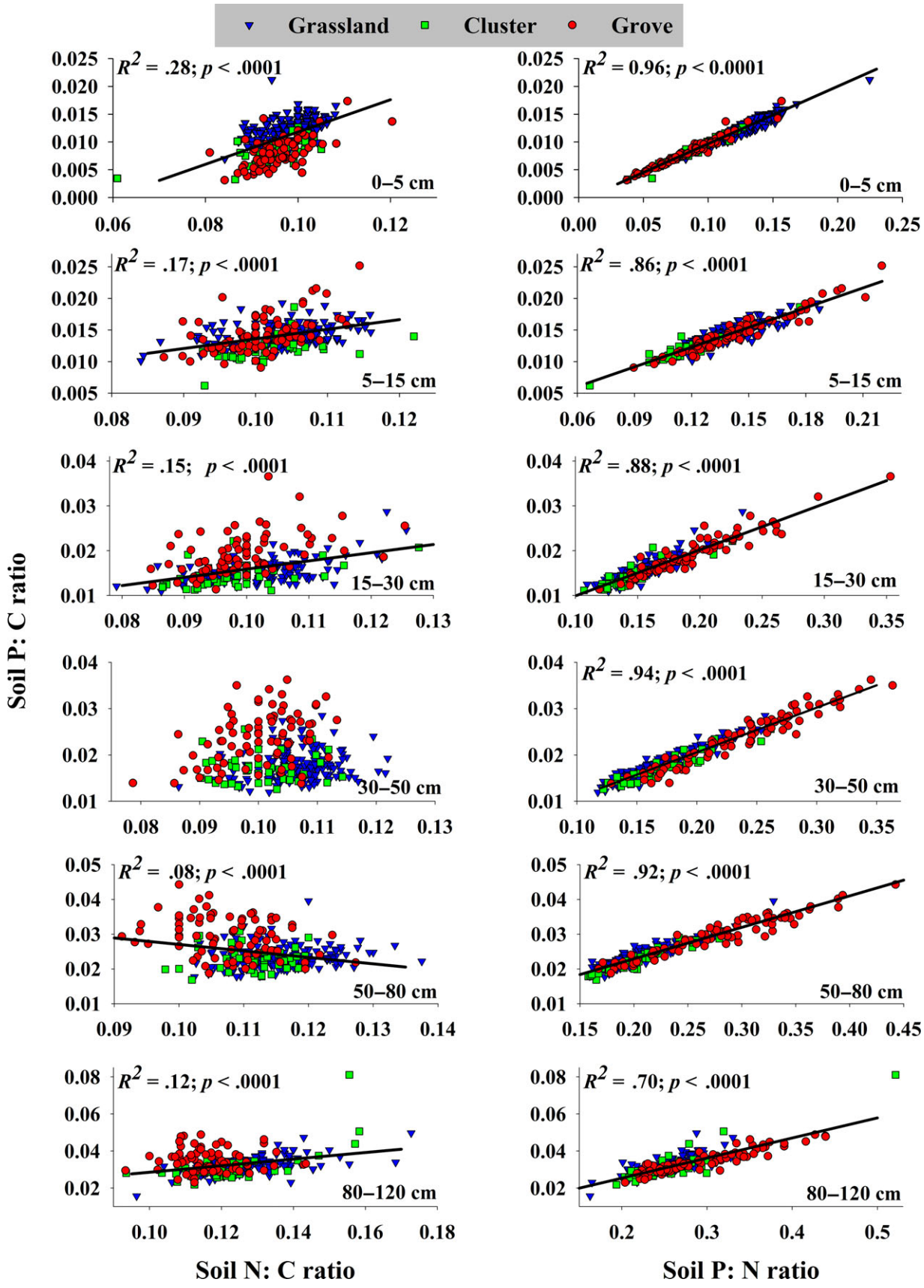


**FIGURE 4** Element ratios plotted against each other for all 320 sampling points across this landscape and throughout the soil profile. Grassland = 200, cluster = 41, and grove = 79 [Colour figure can be viewed at wileyonlinelibrary.com]

| Depth (cm) | Grassland Slope | $r^2$ | Cluster Slope | $r^2$ | Grove Slope | $r^2$ |
|---|---|---|---|---|---|---|
| (a) N-C stoichiometric relationships | | | | | | |
| 0–5 | 0.93 (0.90, 0.96) | .96 | 0.92 (0.86, 0.97) | .97 | 0.96 (0.94, 0.98) | .99 |
| 5–15 | 0.94 (0.89, 0.99) | .84 | 0.91 (0.85, 0.97) | .96 | 0.96 (0.91, 1.01) | .95 |
| 15–30 | 0.87 (0.80, 0.94) | .68 | 0.92 (0.78, 1.08) | .75 | 0.93 (0.84, 1.03) | .81 |
| 30–50 | 0.98 (0.93, 1.04) | .85 | 1.10 (0.96, 1.26) | .82 | 0.94 (0.86, 1.02) | .86 |
| 50–80 | 0.91 (0.85, 0.96) | .83 | 0.96 (0.85, 1.07) | .88 | 1.11 (1.02, 1.20) | .86 |
| 80–120 | 0.79 (0.74, 0.84) | .83 | 0.76 (0.69, 0.85) | .89 | 0.84 (0.78, 0.93) | .85 |
| (b) P-C stoichiometric relationships | | | | | | |
| 0–5 | 0.52 (0.48, 0.56) | .66 | 0.43 (0.37, 0.51) | .76 | 0.50 (0.44, 0.56) | .71 |
| 5–15 | 0.75 (0.58, 0.84) | .42 | 0.58 (0.48, 0.70) | .64 | 1.00 (0.85, 1.18) | .47 |
| 15–30 | 0.88 (0.77, 1.01) | .07 | 0.86 (0.64, 1.15) | .16 | 1.46 (1.20, 1.78) | .23 |
| 30–50 | 0.77 (0.67, 0.89) | .02 | 0.86 (0.63, 1.18) | .02 | 1.17 (0.94, 1.45) | .08 |
| 50–80 | 0.87 (0.77, 0.98) | .23 | 0.73 (0.54, 0.98) | .12 | 1.32 (1.08, 1.60) | .23 |
| 80–120 | 0.54 (0.50, 0.59) | .62 | 0.46 (0.36, 0.58) | .48 | 0.98 (0.82, 1.18) | .35 |

Number of samples: overall = 320, grassland = 200, cluster = 41, and grove = 79.

**TABLE 2** Summary of reduced major axis (RMA) regression analyses for the $\log_{10}$-transformed N-C (a) and P-C (b) stoichiometric relationships across this landscape and throughout the soil profile. Numbers in parentheses are 95% confidence intervals for the slopes of N-C and P-C stoichiometric relationships. If the 95% confidence intervals of the slope include 1.0, it indicates that the slope of N-C or P-C stoichiometric relationship is not significantly different from 1.0

phosphatase activity enabling them to acquire soil P present in organic form (Blaser et al., 2014; Houlton, Wang, Vitousek, & Field, 2008; Olde Venterink, 2011). However, percent increases of P concentrations in leaf and fine root tissues from grasses and woody species were substantially lower than those of N (Figure 3, Appendix S2), and leaf N: P ratios of woody species (24.5 and 27.2 for non-$N_2$ fixers and $N_2$ fixers, respectively) were markedly higher than 16.0 (leaf N: P ratios >16.0 frequently signify P limitations, Aerts & Chapin, 1999; Koerselman & Meuleman, 1996). Therefore, encroaching woody species appear to be more limited by P rather than N.

Without considering the relative abundance of each plant species (Sterner & Elser, 2002) and resorption processes during organ senescence (Reed, Townsend, Davidson, & Cleveland, 2012), results emerging from the leaf and fine root analyses discussed above may not represent the resource stoichiometry of detritus inputs into the soil. However, C-N-P stoichiometry of leaf and fine root tissues could still provide clues about the potential mechanisms underlying the observed C-N-P imbalance in surface soils. The dynamics of soil C, N, and P in surface soils are predominately regulated by biotic factors (e.g., plant residues in the form of leaf litter and dead roots, and the structure and function of microbial communities; Zechmeister-Boltenstern et al., 2015), and may mimic the changes in plant stoichiometric composition following vegetation change (Sistla & Schimel, 2012). Our SEM analyses also showed that fine root density as a biotic factor explained much of the variation in SOC, TN, and TP in the 0–5 cm depth increment across this landscape (Figures 6a and 7a). Thus, the proportionally lower accumulation of soil TP compared to SOC and TN in surface soils might be linked to the fact that this system is limited by P, which in turn causes (1) lower deposition of P to surface soils from woody plant residues compared to N (Figure 3) and (2) more efficient use of P through the active cycling of soil organic P pools (Boutton et al., 2009; Cleveland & Liptzin, 2007). This result was consistent with a global review (Cleveland & Liptzin, 2007) which synthesized 186 observations from surface soils (0–10 cm) and suggested that soil C and N concentrations become increasingly decoupled from soil P concentrations when organic matter accumulates in an ecosystem.

## 4.2 | Soil C-N-P imbalance in subsurface soils following woody encroachment

Soil physicochemical properties gradually surpassed the impact of biotic factors on the accumulations of SOC, TN, and TP with increasing soil depth (Figures 6 and 7), especially in the 30–50 cm depth increment where clay and carbonate C start to accumulate (Appendix S1; Zhou, Boutton, Wu, & Yang, 2017), leading to relatively greater increases in TP compared to SOC and TN in subsurface soils (Tables 1 and 2) and correspondingly distinctive spatial patterns of TP (Figure 5). Soil organic C and N dynamics tend to be strongly coupled and linked primarily through biological processes such as primary production and subsequent microbial mineralization (Delgado-Baquerizo et al., 2013); thus, net accumulations of SOC and TN reflect the balance of SOM inputs and losses (Six et al., 2002). As the main source of SOM input in subsoil (Rumpel & Kögel-Knabner, 2011), root biomass generally decreases exponentially with depth (Jackson et al., 1996). Within this general trend, however, fine root biomass underneath groves was still two times higher than that of grasslands in subsurface soils (Zhou, Boutton, & Wu, 2017).

Surprisingly, SOC and TN in groves did not appear to be substantially higher than grasslands in subsurface soils (Table 1). One explanation for this discrepancy may be ascribed to the physical accessibility of SOM (Dungait, Hopkins, Gregory, & Whitmore, 2012;

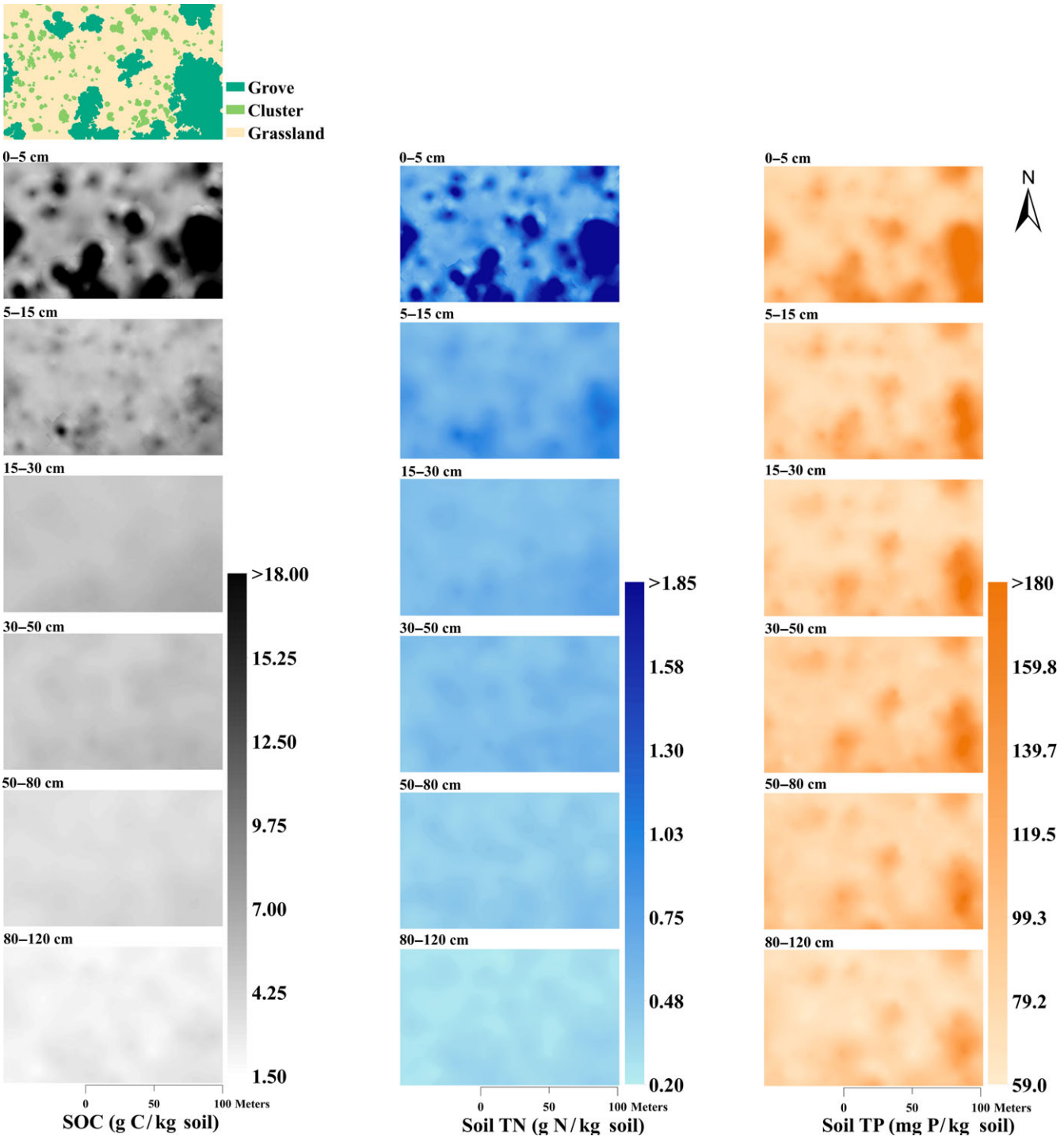


**FIGURE 5** Classified vegetation map of this 160 m × 100 m landscape and kriged maps of soil organic carbon (SOC), total nitrogen (TN), and total phosphorus (TP) throughout the soil profile based on 320 randomly located sampling points. Note that the units for soil TP (mg P $kg^{-1}$ soil) are different than those used for SOC (g C $kg^{-1}$ soil) and TN (g N $kg^{-1}$ soil) [Colour figure can be viewed at wileyonlinelibrary.com]

Salome, Nunan, Pouteau, Lerch, & Chenu, 2010; Six et al., 2002). Across this landscape, groves occupy nonargillic inclusions, whereas grasslands are present on subsurface soils with an argillic horizon (Appendix S1; Archer, 1995; Zhou, Boutton, Wu, & Yang, 2017). Although organic matter inputs via root turnover in subsurface soils of grasslands are low, they may be more effectively physically protected from microbial decomposition by association with fine mineral particles (i.e., clay and silt) that are abundant in subsoils. In contrast, while organic matter inputs in subsurface soils of groves are high, this may be counterbalanced by less physical protection from decomposers due to coarse-textured subsoils. The net outcome is reduced differences in subsoil SOC and TN between groves and

grasslands (Table 1). This explanation for the role of fine mineral particles in regulating the accumulation of SOC and TN may be supported by SEMs, showing that clay and silt content emerged as the main factor explaining the variances of SOC and TN in subsurface soils (Figures 6 and 7). These smaller discrepancies lead to lower level of spatial heterogeneity in SOC and TN across this landscape (Zhou, Boutton, & Wu, 2017), resulting in spatial patterns of SOC and TN in subsurface soils that bear little resemblance to vegetation cover (Figure 5).

While soil organic P is stabilized together with organic C and N and subsequently mineralized through biological processes, the unique geochemical attributes of P cycling allow the fate of mineralized P to differ from C and N (Schlesinger & Bernhardt, 2013). Coarse-textured subsurface soils underneath groves could favor the mineralization of organic matter as discussed above. Mineralized C and N, ultimately, leave the soil profile via gas emissions (e.g., $CO_2$, $N_2$, and nitrogen oxides), plant uptake (e.g., $NO_3^-$ and $NH_4^+$), and leaching. In contrast, mineralized P underneath groves may be immobilized not only by biological uptake but also via the formation of calcium phosphates in basic subsurface soils, as suggested in other studies in dryland environments (Carreira et al., 2006; Ippolito et al., 2010). This interpretation is supported by our findings that (1) soil pH is the dominant factor explaining the variance of TP in subsurface soils (Figures 6 and 7), and (2) carbonate C in subsurface soils beneath groves is higher than that beneath grasslands by up to one order of magnitude and is positively correlated with soil TP (Appendix S6). In addition, separate SEMs including soil carbonate C as an explanatory variable for soil depths below 30 cm where carbonate C starts to accumulate also suggest that soil pH and carbonate C are the primary variables explaining the variance in soil TP, especially for the 30–50 cm depth increment (Appendix S7). This potential P retention in the form of calcium phosphates may lead to a relatively greater increase in TP compared to SOC and TN in subsurface soils (Tables 1 and 2), and substantial increases of TP under groves throughout the soil profile that creates spatial patterns of TP that resemble vegetation pattern across this landscape (Figure 5).

### 4.3 | Implications for soil biogeochemistry following vegetation change

Given the geographic extent of woody encroachment on a global scale (Archer, 2010; Eldridge et al., 2011; Stevens, Lehmann, Murphy, & Durigan, 2017), imbalanced relationships between soil C, N, and P can have important implications for regional and global biogeochemistry and climate. Previous estimates suggest that woody encroachment results in C sequestration (Barger et al., 2011), and represents 20%–40% of the US C sink strength (Houghton, Hackler, & Lawrence, 2000; Pacala et al., 2001; King et al., 2007). In addition, recent studies have reported that significant C accumulation following woody encroachment occurs in deeper portions of the soil profile, suggesting previous estimates may substantially underestimate the role this vegetation change plays in regional and global C sequestration (Chiti et al., 2017; Zhou, Boutton, & Wu, 2017). However, will the C storage potential of dryland ecosystems that are experiencing woody encroachment be ultimately constrained by nutrient limitation, particularly by the key nutrients N and P?

In areas where the encroaching woody plants are capable of symbiotic N fixation, N accrual may be able to increase proportionally with SOC, as observed in this study. Where encroaching woody species are incapable of N fixation, the rate of SOC accrual may become proportionally greater than that of N if plant-available soil N becomes limiting. Given that soil P is generally present in limiting quantities in dryland ecosystems, this may limit the productivity of encroaching woody species, thereby constraining the strength of the carbon sink associated with woody encroachment. In addition, P is a key element in the N-fixation process, and reduced P availability could limit nodulation and reduce fixation rates (Israel, 1987). Thus, the carbon sink strength associated with woody plant encroachment may be tightly linked to concomitant changes in the storage and availability of soil N and P.

Land cover/land use changes often perturb soil biogeochemistry and are considered essential components of coupled biogeochemistry and climate models. Recent studies have recognized the importance of incorporating P cycling into coupled climate–carbon cycling models (Reed, Yang, & Thornton, 2015) and C–N–P interactions into ecosystem models (Achat, Augusto, Gallet-Budynek, & Loustau, 2016). Our findings suggest that modelers should be aware of the fact that the biogeochemical controls over C and N vs. P cycling following vegetation change may be different, and decoupling of P cycling from C and N cycling may lead to differential responses to future perturbations and changes, as shown in this study and others (Delgado-Baquerizo et al., 2013; Jiao et al. 2016). Specific drivers and mechanisms of P cycling should be captured in model development (Achat et al., 2016; Reed et al., 2015), especially when subsurface soils are considered.

**FIGURE 6** Structural equation models showing influences of fine root density, soil clay and silt content, and soil pH on the accumulation of soil organic carbon (SOC), total nitrogen (TN), and total phosphorus (TP) throughout the soil profile following woody plant encroachment, and also correlations between SOC, TN, and TP throughout the soil profile. All variables are observed variables. Single-headed arrows point in the direction of causality, and double-headed arrows indicate correlations between variables. Numbers adjacent to arrows are standardized path coefficients. Continuous and dashed arrows represent positive and negative relationships, respectively, and arrow width is proportional to the strength of the standardized path coefficients. The proportion of variance explained ($R^2$) is shown alongside each response variable. See the a priori conceptual structural equation model in Figure 2. Models for each soil depth were developed based on the combined data for grasslands, clusters, and groves ($N$ = 320 samples/depth) [Colour figure can be viewed at wileyonlinelibrary.com]

(a) 0–5 cm

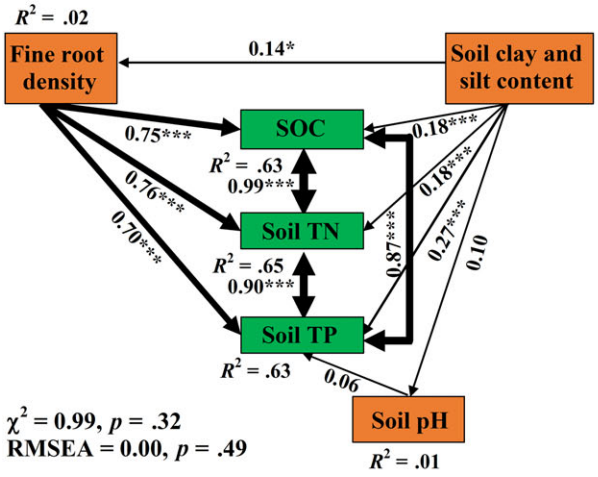


(b) 5–15 cm

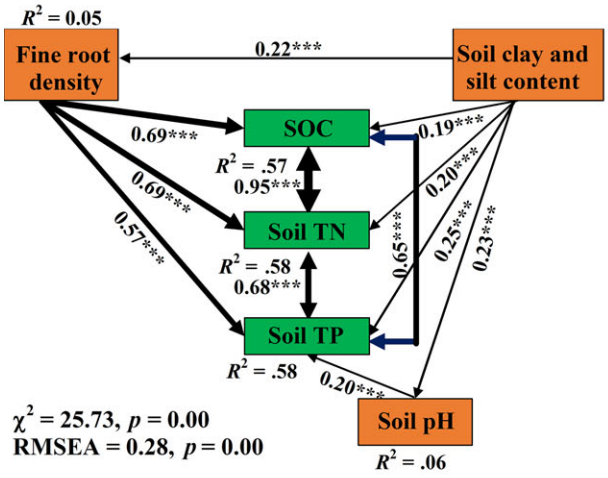


(c) 15–30 cm

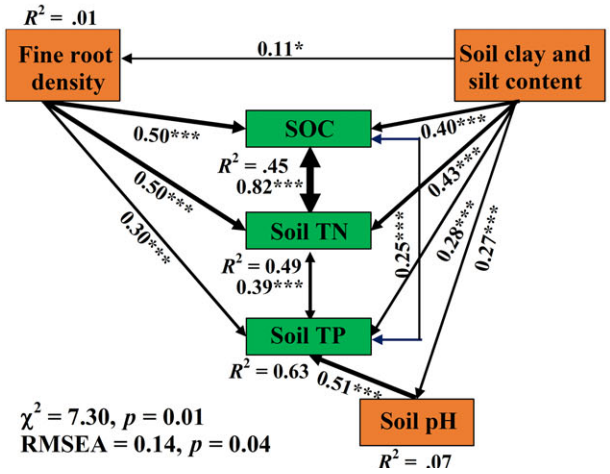


(d) 30– 50 cm

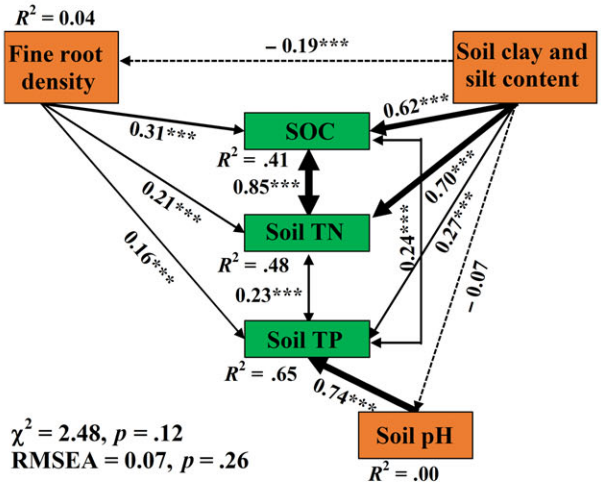


(e) 50–80 cm

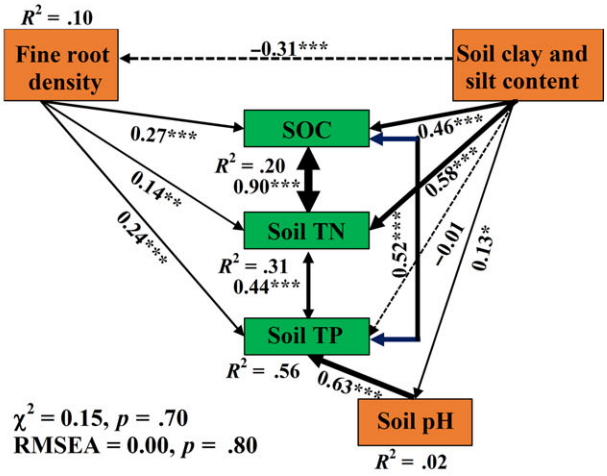


(f) 80–120 cm

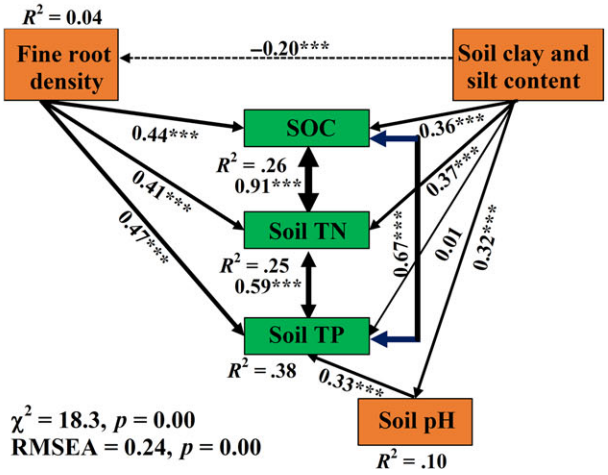

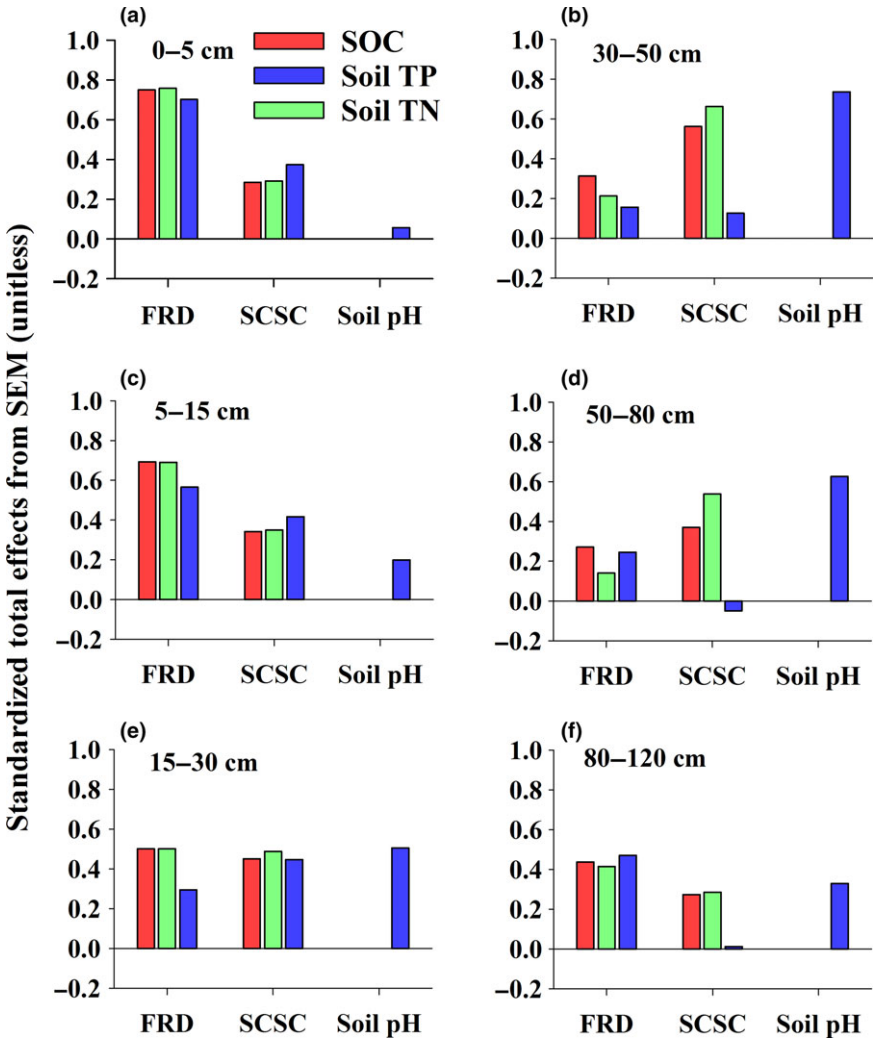


**FIGURE 7** Standardized total effects (direct plus indirect effects) derived from the structural equation models. These include the effects of fine root density (FRD), soil clay and silt content (SCSC), and soil pH on the accumulation of soil organic carbon (SOC), total nitrogen (TN), and total phosphorus (TP) throughout the soil profile following woody encroachment. See Figure 2 for a description of the a priori model, and Figure 5 for the full graphical representation of the six structural equation models developed for each depth increment throughout the soil profile [Colour figure can be viewed at wileyonlinelibrary.com]

In conclusion, we found that SOC and TN were coupled with respect to increasing magnitudes and spatial patterns throughout the soil profile following woody encroachment, whereas TP increased slower than SOC and TN in surface soils but faster in subsurface soils. This imbalanced relationship is likely due to differences in the biotic/abiotic mechanisms that control C and N vs. P accumulation, and to variation in the relative importance of these mechanisms with depth in the soil profile. Simple SEM models showed that C, N, and P concentrations in surface soils were most strongly related to fine root density, whereas in deeper portions of the soil profile the concentrations of those elements were more strongly related to soil texture and pH. Our study highlights the complex response of soil C, N, and P to vegetation change and has far reaching implication for empirical and modeling studies related to the biogeochemistry of dryland ecosystems which are particularly fragile with respect to anticipated global changes.

## ACKNOWLEDGEMENTS

This research was supported by a Doctoral Dissertation Improvement Grant from the U.S. National Science Foundation (DEB/DDIG1600790), an Exploration Fund Grant from the Explorers Club, a Howard McCarley Student Research Award from the Southwestern Association of Naturalists, a Graduate Student Research Grant from Department of Ecosystem Science and Management at Texas A&M University, and by USDA/NIFA (Hatch Project 1003961). Y. Zhou was supported by a Sid Kyle Graduate Merit Assistantship from the Department of Ecosystem Science and Management and a Tom Slick Graduate Research Fellowship from the College of Agriculture and Life Science, Texas A&M University. Comments from Fiona M. Soper helped to improve the manuscript. We thank Ayumi Hyodo for technical support in the Stable Isotopes for Biosphere Sciences Lab at Texas A&M University, and David and Stacy McKown for on-

site logistics at the La Copita Research Area. We also thank three anonymous reviewers for helpful comments, and the editors at *Global Change Biology*. Y. Z., T.W.B., and X.B.W. formulated the original idea and developed methodology; Y. Z. and T.W.B. interpreted the data; Y.Z. performed sample processing and statistical analysis, wrote the first draft of the manuscript, and all authors contributed substantially to revisions.

## ORCID

*Yong Zhou* http://orcid.org/0000-0003-2546-8462
*Thomas W. Boutton* http://orcid.org/0000-0002-7522-5728
*X. Ben Wu* http://orcid.org/0000-0001-5947-3118

## REFERENCES

Achat, D. L., Augusto, L., Gallet-Budynek, A., & Loustau, D. (2016). Future challenges in coupled C–N–P cycle models for terrestrial ecosystems under global change: A review. *Biogeochemistry*, *131*, 173–202. https://doi.org/10.1007/s10533-016-0274-9

Aerts, R., & Chapin, F. S. (1999). The mineral nutrition of wild plants revisited: A re-evaluation of processes and patterns. *Advances in Ecological Research*, *30*, 1–67.

Archer, S. (1995). Tree-grass dynamics in a *Prosopis*-thornscrub savanna parkland: Reconstructing the past and predicting the future. *Ecoscience*, *2*, 83–99. https://doi.org/10.1080/11956860.1995.11682272

Archer, S. R. (2010). Rangeland conservation and shrub encroachment: New perspectives on an old problem. In J. du Toit, R. Kock, & J. Deutsch (Eds.), *Wild rangelands: Conserving wildlife while maintaining livestock in semi-arid ecosystems* (pp. 53–97). Oxford, UK: Wiley-Blackwell. https://doi.org/10.1002/9781444317091

Archer, S., Scifres, C., Bassham, C. R., & Maggio, R. (1988). Autogenic succession in a subtropical savanna: Conversion of grassland to thorn woodland. *Ecological Monographs*, *58*, 111–127. https://doi.org/10.2307/1942463

Bai, E., Boutton, T. W., Liu, F., Wu, X. B., & Archer, S. R. (2012). Spatial patterns of soil $\delta^{13}C$ reveal grassland-to-woodland successional processes. *Organic Geochemistry*, *42*, 1512–1518. https://doi.org/10.1016/j.orggeochem.2010.11.004

Bai, E., Boutton, T. W., Liu, F., Wu, X. B., Archer, S. R., & Hallmark, C. T. (2008). Spatial variation of $\delta^{15}N$ of woody plants along a topoedaphic gradient in a subtropical savanna. *Oecologia*, *159*, 493–503.

Barger, N. N., Archer, S. R., Campbell, J. L., Huang, C. Y., Morton, J. A., & Knapp, A. K. (2011). Woody plant proliferation in North American drylands: A synthesis of impacts on ecosystem carbon balance. *Journal of Geophysical Research: Biogeosciences*, *116*, G00K07. https://doi.org/10.1029/2010JG001506

Blaser, W. J., Shanungu, G. K., Edwards, P. J., & Olde Venterink, H. (2014). Woody encroachment reduces nutrient limitation and promotes soil carbon sequestration. *Ecology and Evolution*, *4*, 1423–1438. https://doi.org/10.1002/ece3.1024

Boutton, T. W., Archer, S. R., Midwood, A. J., Zitzer, S. F., & Bol, R. (1998). $\delta^{13}C$ values of soil organic carbon and their use in documenting vegetation change in a subtropical savanna ecosystem. *Geoderma*, *82*, 5–41. https://doi.org/10.1016/S0016-7061(97)00095-5

Boutton, T. W., Kantola, I. B., Stott, D. E., Balthrop, S. L., Tribble, J. E., & Filley, T. R. (2009). Soil phosphatase activity and plant available phosphorus increase following grassland invasion by N-fixing tree legumes. *Eos Transactions of the American Geophysical Union*, *90*(52), B21B–0338.

Boutton, T. W., & Liao, J. D. (2010). Changes in soil nitrogen storage and $\delta^{15}N$ with woody plant encroachment in a subtropical savanna parkland landscape. *Journal of Geophysical Research: Biogeosciences*, *115*, G03019. https://doi.org/10.1029/2009JG001184

Carreira, J. A., Vinegla, B., & Lajtha, K. (2006). Secondary $CaCO_3$ and precipitation of P-Ca compounds control the retention of soil P in arid ecosystems. *Journal of Arid Environments*, *64*, 460–473. https://doi.org/10.1016/j.jaridenv.2005.06.003

Chiti, T., Mihindou, V., Jeffery, K. J., Malhi, Y., De Oliveira, F. L., White, L. J. & Valentini, R. (2017). Impact of woody encroachment on soil organic carbon storage in the Lopé National Park, Gabon. *Biotropica*, *49*, 9–13. https://doi.org/10.1111/btp.12369

Cleveland, C. C., & Liptzin, D. (2007). C: N: P stoichiometry in soil: Is there a "Redfield ratio" for the microbial biomass? *Biogeochemistry*, *85*, 235–252. https://doi.org/10.1007/s10533-007-9132-0

Delgado-Baquerizo, M., Maestre, F. T., Gallardo, A., Bowker, M. A., Wallenstein, M. D., Quero, J. L., ... Zaady, E. (2013). Decoupling of soil nutrient cycles as a function of aridity in global drylands. *Nature*, *502*, 672–676. https://doi.org/10.1038/nature12670

Dungait, J. A., Hopkins, D. W., Gregory, A. S., & Whitmore, A. P. (2012). Soil organic matter turnover is governed by accessibility not recalcitrance. *Global Change Biology*, *18*, 1781–1796. https://doi.org/10.1111/j.1365-2486.2012.02665.x

Eldridge, D. J., Bowker, M. A., Maestre, F. T., Roger, E., Reynolds, J. F., & Whitford, W. G. (2011). Impacts of shrub encroachment on ecosystem structure and functioning: Towards a global synthesis. *Ecology Letters*, *14*, 709–722. https://doi.org/10.1111/j.1461-0248.2011.01630.x

Elser, J., & Bennett, E. (2011). Phosphorus cycle: A broken biogeochemical cycle. *Nature*, *478*, 29–31. https://doi.org/10.1038/478029a

Elser, J. J., Fagan, W. F., Kerkhoff, A. J., Swenson, N. G., & Enquist, B. J. (2010). Biological stoichiometry of plant production: Metabolism, scaling and ecological response to global change. *New Phytologist*, *186*, 593–608. https://doi.org/10.1111/j.1469-8137.2010.03214.x

Grace, J. B. (2006). *Structural equation modeling and natural systems*. Cambridge, UK: Cambridge University Press. https://doi.org/10.1017/CBO9780511617799

Harris, D., Horwáth, W. R., & van Kessel, C. (2001). Acid fumigation of soils to remove carbonates prior to total organic carbon or carbon-13 isotopic analysis. *Soil Science Society of America Journal*, *65*, 1853–1856. https://doi.org/10.2136/sssaj2001.1853

Hessen, D. O., Ågren, G. I., Anderson, T. R., Elser, J. J., & de Ruiter, P. C. (2004). Carbon sequestration in ecosystems: The role of stoichiometry. *Ecology*, *85*, 1179–1192. https://doi.org/10.1890/02-0251

Hibbard, K. A., Schimel, D. S., Archer, S., Ojima, D. S., & Parton, W. (2003). Grassland to woodland transitions: Integrating changes in landscape structure and biogeochemistry. *Ecological Applications*, *13*, 911–926. https://doi.org/10.1890/1051-0761(2003)13[911:GTWTIC]2.0.CO;2

Houghton, R. A., Hackler, J. L., & Lawrence, K. T. (1999). The US carbon budget: Contributions from land-use change. *Science*, *285*, 574–578. https://doi.org/10.1126/science.285.5427.574

Houghton R. A, Hackler J. L., & Lawrence K. T. (2000). Changes in terrestrial carbon storage in the United States 2: The role of fire and fire management. *Global Ecology and Biogeography*, *9*, 145–170.

Houlton, B. Z., Wang, Y. P., Vitousek, P. M., & Field, C. B. (2008). A unifying framework for dinitrogen fixation in the terrestrial biosphere. *Nature*, *454*, 327–330. https://doi.org/10.1038/nature07028

Hughes, R. F., Archer, S. R., Asner, G. P., Wessman, C. A., McMurtry, C., Nelson, J. & Ansley, R. J. (2006). Changes in aboveground primary production and carbon and nitrogen pools accompanying woody plant encroachment in a temperate savanna. *Global Change Biology*, *12*, 1733–1747. https://doi.org/10.1111/j.1365-2486.2006.01210.x

Ippolito, J. A., Blecker, S. W., Freeman, C. L., McCulley, R. L., Blair, J. M., & Kelly, E. F. (2010). Phosphorus biogeochemistry across a precipitation gradient in grasslands of central North America. *Journal of Arid*

*Environments*, *74*, 954–961. https://doi.org/10.1016/j.jaridenv.2010.01.003

Israel, D. W. (1987). Investigation of the role of phosphorus in symbiotic dinitrogen fixation. *Plant Physiology*, *84*, 835–840. https://doi.org/10.1104/pp.84.3.835

Jackson, R. B., Canadell, J., Ehleringer, J. R., Mooney, H. A., Sala, O. E., & Schulze, E. D. (1996). A global analysis of root distributions for terrestrial biomes. *Oecologia*, *108*, 389–411. https://doi.org/10.1007/BF00333714

Jiao, F., Shi, X. R., Han, F. P., & Yuan, Z. Y. (2016). Increasing aridity, temperature and soil pH induce soil C-N-P imbalance in grasslands. *Scientific Reports*, *6*, 19601. https://doi.org/10.1038/srep19601

Kantola, I. B. (2012). *Biogeochemistry of woody plant invasion: Phosphorus cycling and microbial community composition*. Doctoral dissertation, Texas A&M University, College Station, TX.

King, A. W., Dilling, L., Zimmerman, G. P., Fairman, D. M., Houghton, R. A., Marland, G., … Wilbanks, T. J. (2007) Executive summary. In A. W. King, L. Dilling, G. P. Zimmerman, D. M. Fairman, R. A. Houghton, G. Marland, A. Z. Rose & T. J. Wilbanks (Eds.), *The First State of the Carbon Cycle Report (SOCCR): The North American Carbon Budget and Implications for the Global Carbon Cycle*. A Report by the U.S. Climate Change Science Program and the Subcommittee on Global Change Research (pp. 1–14). Asheville, NC: National Oceanic and Atmospheric Administration, National Climatic Data Center.

Koerselman, W., & Meuleman, A. F. (1996). The vegetation N: P ratio: A new tool to detect the nature of nutrient limitation. *Journal of Applied Ecology*, *33*, 1441–1450. https://doi.org/10.2307/2404783

Lajtha, K., Driscoll, C. T., Jarrell, W. M., & Elliott, E. T. (1999) Soil phosphorus: Characterization and total element analysis. In G. P. Roberts, D. C. Coleman, C. S. Bledsoe & P. Sollins (Eds.), *Standard soil methods for long-term ecological research* (pp. 115–142). New York, NY: Oxford University Press.

Li, H., Shen, H., Chen, L., Liu, T., Hu, H., Zhao, X., … Fang, J. (2016). Effects of shrub encroachment on soil organic carbon in global grasslands. *Scientific Reports*, *6*, 28974. https://doi.org/10.1038/srep28974

Littell, R. C., Stroup, W. W., Milliken, G. A., Wolfinger, R. D., & Schabenberger, O. (2006). *SAS for mixed models*. Cary, NC: SAS Institute.

Liu, F., Wu, X., Bai, E., Boutton, T. W., & Archer, S. R. (2010). Spatial scaling of ecosystem C and N in a subtropical savanna landscape. *Global Change Biology*, *16*, 2213–2223.

Liu, F., Wu, X., Bai, E., Boutton, T. W., & Archer, S. R. (2011). Quantifying soil organic carbon in complex landscapes: An example of grassland undergoing encroachment of woody plants. *Global Change Biology*, *17*, 1119–1129. https://doi.org/10.1111/j.1365-2486.2010.02251.x

Maestre, F. T., Bowker, M. A., Puche, M. D., Belén Hinojosa, M., Martínez, I., García-Palacios, P., … Escudero, A. (2009). Shrub encroachment can reverse desertification in semi-arid Mediterranean grasslands. *Ecology Letters*, *12*, 930–941. https://doi.org/10.1111/j.1461-0248.2009.01352.x

McCulley, R. L., Archer, S. R., Boutton, T. W., Hons, F. M., & Zuberer, D. A. (2004). Soil respiration and nutrient cycling in wooded communities developing in grassland. *Ecology*, *85*, 2804–2817. https://doi.org/10.1890/03-0645

McGroddy, M. E., Daufresne, T., & Hedin, L. O. (2004). Scaling of C: N: P stoichiometry in forests worldwide: Implications of terrestrial Redfield-type ratios. *Ecology*, *85*, 2390–2401. https://doi.org/10.1890/03-0351

Murphy, J., & Riley, J. P. (1962). A modified single solution method for the determination of phosphate in natural waters. *Analytica Chimica Acta*, *27*, 31–36. https://doi.org/10.1016/S0003-2670(00)88444-5

Niklas, K. J., & Cobb, E. D. (2005). N, P, and C stoichiometry of *Eranthis hyemalis* (Ranunculaceae) and the allometry of plant growth. *American Journal of Botany*, *92*, 1256–1263. https://doi.org/10.3732/ajb.92.8.1256

Olde Venterink, H. (2011). Legumes have a higher root phosphatase activity than other forbs, particularly under low inorganic P and N supply. *Plant and Soil*, *347*, 137–146. https://doi.org/10.1007/s11104-011-0834-7

Pacala, S. W., Hurtt, G. C., Baker, D., Peylin, P., Houghton, R. A., Birdsey, R. A., … Field, C. B. (2001). Consistent land-and atmosphere-based US carbon sink estimates. *Science*, *292*, 2316–2320. https://doi.org/10.1126/science.1057320

Peñuelas, J., Sardans, J., Rivas-ubach, A., & Janssens, I. A. (2012). The human-induced imbalance between C, N and P in Earth's life system. *Global Change Biology*, *18*, 3–6. https://doi.org/10.1111/j.1365-2486.2011.02568.x

Redfield, A. C. (1958). The biological control of chemical factors in the environment. *American Scientist*, *46*, 205–221.

Reed, S. C., Townsend, A. R., Davidson, E. A., & Cleveland, C. C. (2012). Stoichiometric patterns in foliar nutrient resorption across multiple scales. *New Phytologist*, *196*, 173–180. https://doi.org/10.1111/j.1469-8137.2012.04249.x

Reed, S. C., Yang, X., & Thornton, P. E. (2015). Incorporating phosphorus cycling into global modeling efforts: A worthwhile, tractable endeavor. *New Phytologist*, *208*, 324–329. https://doi.org/10.1111/nph.13521

Reich, P. B., Walters, M. B., & Ellsworth, D. S. (1997). From tropics to tundra: Global convergence in plant functioning. *Proceedings of the National Academy of Sciences of the United States of America*, *94*, 13730–13734. https://doi.org/10.1073/pnas.94.25.13730

Rumpel, C., & Kögel-Knabner, I. (2011). Deep soil organic matter-a key but poorly understood component of terrestrial C cycle. *Plant and Soil*, *338*, 143–158. https://doi.org/10.1007/s11104-010-0391-5

Salome, C., Nunan, N., Pouteau, V., Lerch, T. Z., & Chenu, C. (2010). Carbon dynamics in topsoil and in subsoil may be controlled by different regulatory mechanisms. *Global Change Biology*, *16*, 416–426. https://doi.org/10.1111/(ISSN)1365-2486

Schenk, H. J., & Jackson, R. B. (2002). Rooting depths, lateral root spreads and below-ground/above-ground allometries of plants in water-limited ecosystems. *Journal of Ecology*, *90*, 480–494. https://doi.org/10.1046/j.1365-2745.2002.00682.x

Schlesinger, W. H., & Bernhardt, E. S. (2013). *Biogeochemistry*. New York, NY: Academic Press. https://doi.org/10.1093/OBO_dataset_home

Schmidt, M. W., Torn, M. S., Abiven, S., Dittmar, T., Guggenberger, G., Janssens, I. A., … Trumbore, S. E. (2011). Persistence of soil organic matter as an ecosystem property. *Nature*, *478*, 49–56. https://doi.org/10.1038/nature10386

Scholes, R. J., & Archer, S. R. (1997). Tree-grass interactions in savannas. *Annual Review of Ecology and Systematics*, *28*, 517–544. https://doi.org/10.1146/annurev.ecolsys.28.1.517

Sheldrick, B. H., & Wang, C. (1993). Particle size distribution. In M. R. Carter (Ed.), *Soil sampling and methods of analysis* (pp. 499–511). Ann Arbor, MI: Lewis Publishers, Canadian Society of Soil Science.

Sistla, S. A., & Schimel, J. P. (2012). Stoichiometric flexibility as a regulator of carbon and nutrient cycling in terrestrial ecosystems under change. *New Phytologist*, *196*, 68–78. https://doi.org/10.1111/j.1469-8137.2012.04234.x

Sitters, J., Edwards, P. J., & Venterink, H. O. (2013). Increases of soil C, N, and P pools along an acacia tree density gradient and their effects on trees and grasses. *Ecosystems*, *16*, 347–357. https://doi.org/10.1007/s10021-012-9621-4

Six, J., Conant, R. T., Paul, E. A., & Paustian, K. (2002). Stabilization mechanisms of soil organic matter: Implications for C-saturation of soils. *Plant and Soil*, *241*, 155–176. https://doi.org/10.1023/A:1016125726789

Soper, F. M., Boutton, T. W., & Sparks, J. P. (2015). Investigating patterns of symbiotic nitrogen fixation during vegetation change from grassland to woodland using fine scale $\delta^{15}N$ measurements. *Plant, Cell and Environment*, *38*, 89–100. https://doi.org/10.1111/pce.12373

Soper, F. M., & Sparks, J. P. (2017). Estimating ecosystem nitrogen addition by a leguminous tree: A mass balance approach using a woody encroachment chronosequence. *Ecosystems*, *20*, 1164–1178. https://doi.org/10.1007/s10021-016-0100-1

Sterner, R. W., & Elser, J. J. (2002). *Ecological stoichiometry: The biology of elements from molecules to the biosphere*. Princeton, NJ: Princeton University Press.

Stevens, N., Lehmann, C. E., Murphy, B. P., & Durigan, G. (2017). Savanna woody encroachment is widespread across three continents. *Global Change Biology*, *23*, 235–244. https://doi.org/10.1111/gcb.13409

Vitousek, P. M., Porder, S., Houlton, B. Z., & Chadwick, O. A. (2010). Terrestrial phosphorus limitation: Mechanisms, implications, and nitrogen–phosphorus interactions. *Ecological Applications*, *20*, 5–15. https://doi.org/10.1890/08-0127.1

Walker, T. W., & Syers, J. K. (1976). The fate of phosphorus during pedogenesis. *Geoderma*, *15*, 1–19. https://doi.org/10.1016/0016-7061(76)90066-5

Yang, Y., & Luo, Y. (2011). Carbon: Nitrogen stoichiometry in forest ecosystems during stand development. *Global Ecology and Biogeography*, *20*, 354–361. https://doi.org/10.1111/j.1466-8238.2010.00602.x

Zechmeister-Boltenstern, S., Keiblinger, K. M., Mooshammer, M., Peñuelas, J., Richter, A., Sardans, J. & Wanek, W. (2015). The application of ecological stoichiometry to plant–microbial–soil organic matter transformations. *Ecological Monographs*, *85*, 133–155. https://doi.org/10.1890/14-0777.1

Zhou, Y., Boutton, T. W., & Wu, X. B. (2017). Soil carbon response to woody plant encroachment: Importance of spatial heterogeneity and deep soil storage. *Journal of Ecology*, *105*, 1738–1749. https://doi.org/10.1111/1365-2745.12770

Zhou, Y., Boutton, T. W., Wu, X. B., & Yang, C. (2017). Spatial heterogeneity of subsurface soil texture drives landscape-scale patterns of woody patches in a subtropical savanna. *Landscape Ecology*, *32*, 915–929. https://doi.org/10.1007/s10980-017-0496-9

Zitzer, S. F., Archer, S. R., & Boutton, T. W. (1996). Spatial variability in the potential for symbiotic $N_2$ fixation by woody plants in a subtropical savanna ecosystem. *Journal of Applied Ecology*, *33*, 1125–1136. https://doi.org/10.2307/2404692

## SUPPORTING INFORMATION

Additional Supporting Information may be found online in the supporting information tab for this article.

**How to cite this article:** Zhou Y, Boutton TW, Wu XB. Soil phosphorus does not keep pace with soil carbon and nitrogen accumulation following woody encroachment. *Glob Change Biol*. 2018;24:1992–2007. https://doi.org/10.1111/gcb.14048

**Appendix S1**

Conceptual model of vegetation cover on upland portions of this area. Small discrete clusters (< 100 $m^2$ in canopy area) are dispersed among herbaceous vegetation where the argillic horizon (Bt) is present, whereas groves (> 100 $m^2$ in canopy area) occupy non-argillic inclusions and expand laterally to the boundary where the argillic horizon begins. Originally published by Zhou et al. (2017), reprinted with permission.

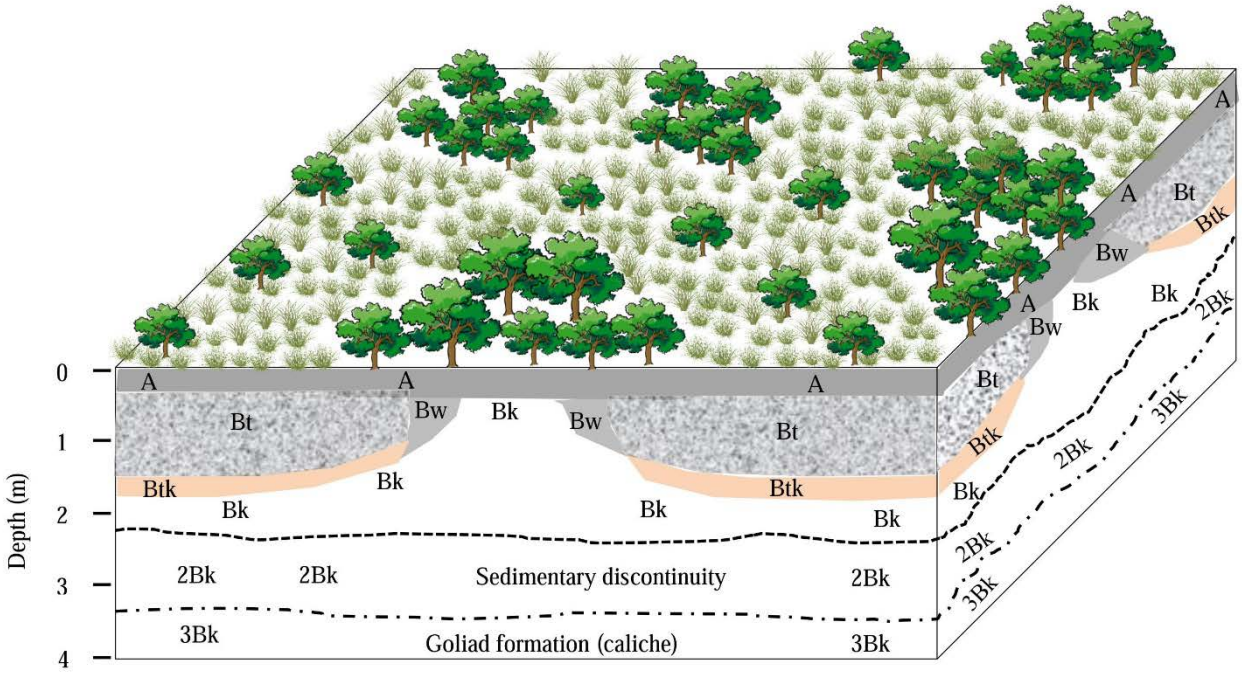

**Appendix S2**

Carbon (C), nitrogen (N) and phosphorus (P) concentrations of leaf and fine root tissues for each plant species across this 160 m × 100 m study area. Leaf and fine root tissues for each woody species were collected from three individuals. For grasses, forbs, and crassulacean acid metabolism (CAM) species, approximately 5-10 individual plants were collected to meet the mass requirement for elemental analyses. Number of non $N_2$-fixing woody species = 13, $N_2$-fixing woody species = 2, forbs = 9, grasses = 13, and CAM species = 3.

| Species name | Leaf tissue | | | | Fine root tissue | | |
|---|---|---|---|---|---|---|---|
| | C conc. (g/kg) | N conc. (g/kg) | P conc. (g/kg) | | C conc. (g/kg) | N conc. (g/kg) | P conc. (g/kg) |
| **Non $N_2$-fixing woody species** | | | | | | | |
| *Bernardia myricifolia* | 426.2 | 30.0 | 1.14 | | 491.5 | 19.0 | 0.62 |
| *Celtis pallida* | 406.9 | 39.9 | 1.14 | | 467.2 | 30.9 | 0.32 |
| *Condalia hookeri* | 456.5 | 20.1 | 0.78 | | 472.8 | 23.8 | 0.54 |
| *Diospyros texana* | 513.4 | 23.1 | 0.82 | | 477.3 | 11.7 | 0.37 |
| *Foresteria angustifolia* | 480.0 | 21.9 | 0.86 | | 482.2 | 10.1 | 0.54 |
| *Karwinskia humboldtiana* | 471.4 | 28.8 | 1.01 | | 484.6 | 10.5 | 0.53 |
| *Lycium berlandieri* | 492.2 | 21.0 | 1.02 | | 491.9 | 10.6 | 0.43 |
| *Mahonia trifoliolata* | 501.6 | 14.4 | 0.89 | | 522.3 | 15.6 | 0.42 |
| *Schaefferia cuneifolia* | 437.0 | 25.3 | 1.18 | | 475.7 | 31.8 | 0.43 |
| *Zanthoxylum fagara* | 483.3 | 25.9 | 1.22 | | 488.5 | 22.5 | 0.56 |
| *Coleogyne ramosissima* | 521.1 | 26.1 | 1.06 | | 535.2 | 16.3 | 0.28 |
| *Salvia ballotiflora* | 480.1 | 25.2 | 1.40 | | 522.9 | 12.0 | 0.46 |
| *Acacia greggii* | 510.1 | 30.2 | 1.12 | | 486.0 | 12.0 | 0.23 |
| **$N_2$-fixing woody species** | | | | | | | |
| *Acacia schaffneri* | 513.1 | 33.5 | 1.20 | | 502.4 | 11.4 | 0.34 |

| | | | | | | | |
|---|---|---|---|---|---|---|---|
| *Prosopis glandulosa* | 510.4 | 40.0 | 1.52 | | 506.9 | 26.7 | 0.64 |
| **Forbs** | | | | | | | |
| *Croton texensis* | 461.9 | 30.4 | 1.42 | | 484.8 | 4.8 | 0.16 |
| *Wedelia texana* | 418.7 | 26.0 | 1.16 | | 500.0 | 7.6 | 0.26 |
| *Aphanostephus riddellii* | 450.2 | 23.2 | 1.21 | | 490.4 | 9.1 | 0.38 |
| *Ambrosia confertiflora* | 475.9 | 31.1 | 1.84 | | 490.8 | 13.3 | 0.43 |
| *Parthenium hysterophorus* | 390.8 | 30.7 | 0.74 | | 481.3 | 6.6 | 0.31 |
| *Palafoxia callosa* | 455.6 | 22.3 | 0.84 | | 493.6 | 4.0 | 0.28 |
| *Amphiachyris amoena* | 493.7 | 26.5 | 1.36 | | 497.7 | 6.2 | 0.33 |
| *Thymophylla pentachaeta* | 429.6 | 21.3 | 1.18 | | 486.2 | 7.0 | 0.37 |
| *Xanthisma texanum* | 485.0 | 27.5 | 1.16 | | 507.5 | 11.8 | 0.64 |
| **Grasses** | | | | | | | |
| *Tridens albescens* | 427.5 | 17.9 | 0.68 | | 516.2 | 8.2 | 0.28 |
| *Setaria texana* | 442.4 | 35.2 | 1.76 | | 479.7 | 13.8 | 0.39 |
| *Bothriochloa ischaemum* | 447.8 | 14.6 | 0.93 | | 466.2 | 3.0 | 0.13 |
| *Aristida purpurea* | 463.3 | 13.9 | 1.06 | | 482.5 | 4.0 | 0.13 |
| *Cenchrus ciliaris* | 426.5 | 24.8 | 1.45 | | 489.7 | 6.4 | 0.23 |
| *Heteropogon contortus* | 444.9 | 15.2 | 0.70 | | 455.9 | 2.9 | 0.14 |
| *Chloris cucullata* | 469.1 | 18.2 | 0.76 | | 508.5 | 4.7 | 0.18 |
| *Eragrostis secundiflora* | 464.5 | 16.8 | 0.80 | | 501.7 | 4.9 | 0.15 |
| *Paspalum setaceum* | 427.6 | 17.8 | 0.93 | | 486.9 | 6.5 | 0.31 |
| *Sporobolus neglectus* | 442.3 | 20.2 | 1.19 | | 515.3 | 4.7 | 0.25 |
| *Bouteloua rigidiseta* | 430.5 | 15.0 | 0.58 | | 497.8 | 4.3 | 0.16 |
| *Bouteloua trifida* | 438.3 | 20.4 | 1.15 | | 475.6 | 6.4 | 0.23 |
| *Panicum hallii* | 442.3 | 20.0 | 0.77 | | 501.9 | 5.5 | 0.22 |
| **CAM species** | | | | | | | |
| *Opuntia engelmannii* | 338.8 | 7.3 | 0.41 | | 461.7 | 8.2 | 0.26 |
| *Cylindropuntia leptocaulis* | 388.1 | 9.4 | 0.53 | | 499.7 | 11.5 | 0.31 |
| *Yucca treculeana* | 445.9 | 18.6 | 1.37 | | 508.9 | 4.0 | 0.16 |

**Appendix S3**

Variogram analysis was used to determine the spatial autocorrelation pattern for SOC, TN, and TP within each soil depth increment. The experimental semivariogram for each soil depth increment was calculated according to:

$$\gamma(h) = \frac{1}{2N(h)} \sum_{i=1}^{i=N(h)} [Z(X_i) - Z(X_{i+h})]^2$$

Where $\gamma(h)$ is semivariance and h is the lag distance. $Z(X_i)$ and $Z(X_{i+h})$ are the values of measured properties (i.e. SOC, TN, and TP) at a spatial location $X_i$ and $X_{i+h}$. N(h) is the number of pairs with lag distance h. Spherical model was fitted to each experimental semivariogram to obtain the nugget ($C_0$), range, partial sill ($C$), and sill ($C_0+C$) for ordinary kriging as summarized in the following table.

| | Depth (cm) | Nugget ($C_0$) | Partial sill ($C$) | Sill ($C_0+C$) | C/( $C_0+C$) (%) | Range (m) | $R^2$ | RMSD |
|---|---|---|---|---|---|---|---|---|
| SOC | 0-5 | 16.42 | 65.28 | 81.70 | 79.90 | 10.64 | 0.23 | 8.50 |
| | 5-15 | 0.64 | 3.38 | 4.02 | 84.08 | 9.27 | 0.18 | 2.04 |
| | 15-30 | 0.51 | 0.34 | 0.85 | 40.00 | 62.26 | 0.35 | 0.79 |
| | 30-50 | 0.38 | 0.19 | 0.57 | 33.33 | 17.55 | 0.22 | 0.73 |
| | 50-80 | 0.13 | 0.10 | 0.23 | 43.48 | 35.57 | 0.36 | 0.43 |
| | 80-120 | 0.09 | 0.17 | 0.26 | 65.38 | 24.96 | 0.42 | 0.42 |
| TN | 0-5 | 0.060 | 0.60 | 0.66 | 90.91 | 10.96 | 0.27 | 0.75 |
| | 5-15 | 0.021 | 0.016 | 0.037 | 43.24 | 22.52 | 0.32 | 0.18 |
| | 15-30 | 0.0033 | 0.0027 | 0.006 | 45.00 | 22.74 | 0.33 | 0.07 |
| | 30-50 | 0.0028 | 0.0027 | 0.0055 | 49.09 | 20.05 | 0.27 | 0.07 |
| | 50-80 | 0.0012 | 0.0015 | 0.0027 | 55.56 | 21.21 | 0.36 | 0.04 |
| | 80-120 | 0.00090 | 0.0014 | 0.0023 | 60.87 | 23.80 | 0.42 | 0.04 |
| TP | 0-5 | 451.38 | 811.36 | 1262.74 | 64.25 | 32.16 | 0.53 | 26.53 |
| | 5-15 | 88.92 | 496.64 | 585.56 | 84.81 | 33.64 | 0.69 | 14.96 |
| | 15-30 | 51.58 | 462.65 | 514.23 | 89.97 | 40.84 | 0.78 | 11.66 |
| | 30-50 | 31.20 | 403.27 | 434.47 | 92.82 | 38.34 | 0.80 | 10.15 |
| | 50-80 | 29.10 | 301.36 | 330.46 | 91.19 | 36.29 | 0.78 | 9.46 |
| | 80-120 | 21.71 | 206.19 | 227.90 | 90.47 | 34.04 | 0.73 | 8.65 |

RMSD represents the root-mean-square deviation.

**Appendix S4**

Predicted slopes for scaling relationships between soil C vs N and C vs P. Line A represents the situation where the slope of the scaling relationship approximates 1, indicating proportional changes between C and N, or C and P in soils. Line B represents that the slope of the scaling relationship is > 1, indicating a situation where N or P change more rapidly than C. In contrast, line C represents that the slope of the scaling relationship is < 1, indicating that N or P change more slowly than C (Adapted from McGroddy et al. 2004).

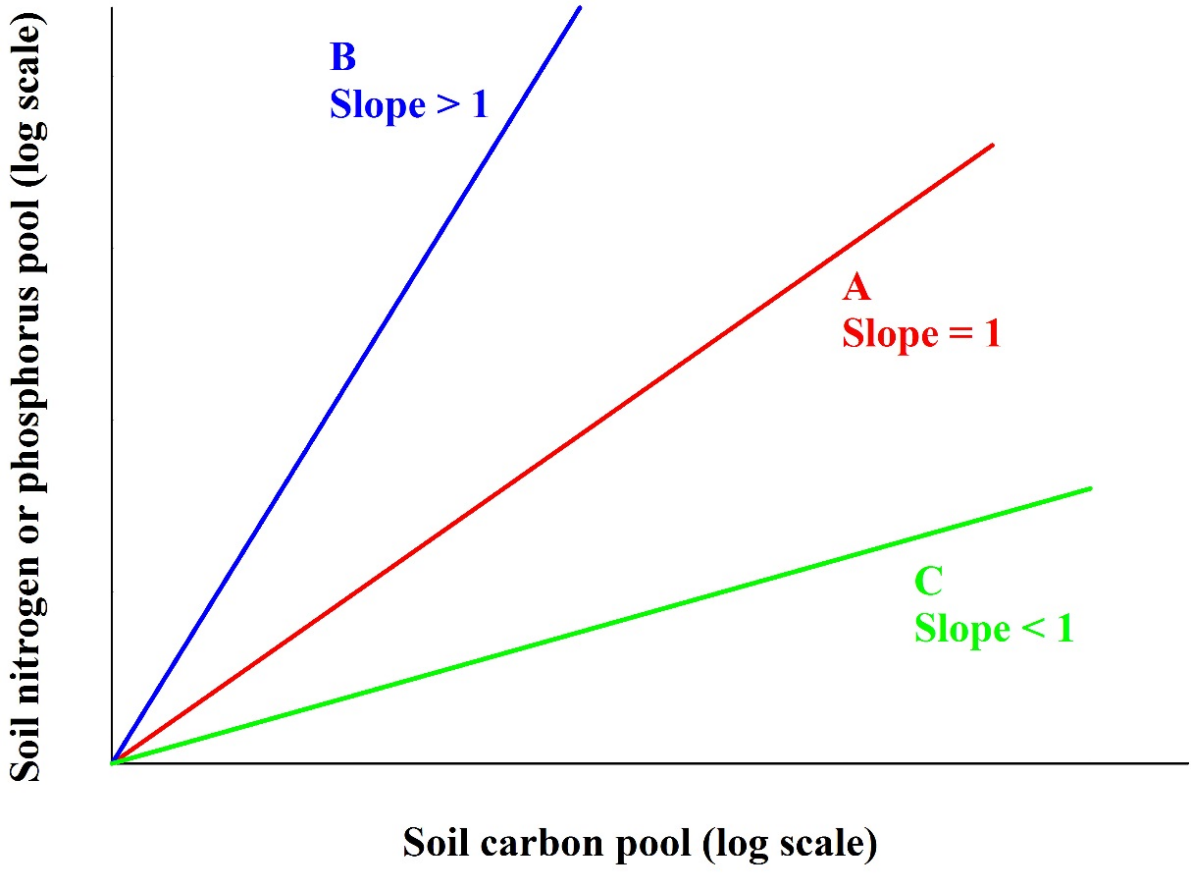

**Appendix S5**

Relationships between soil N: C and P: C ratios for different landscape elements across this landscape and throughout the soil profile. Grassland = 200, cluster = 41, and grove = 79.

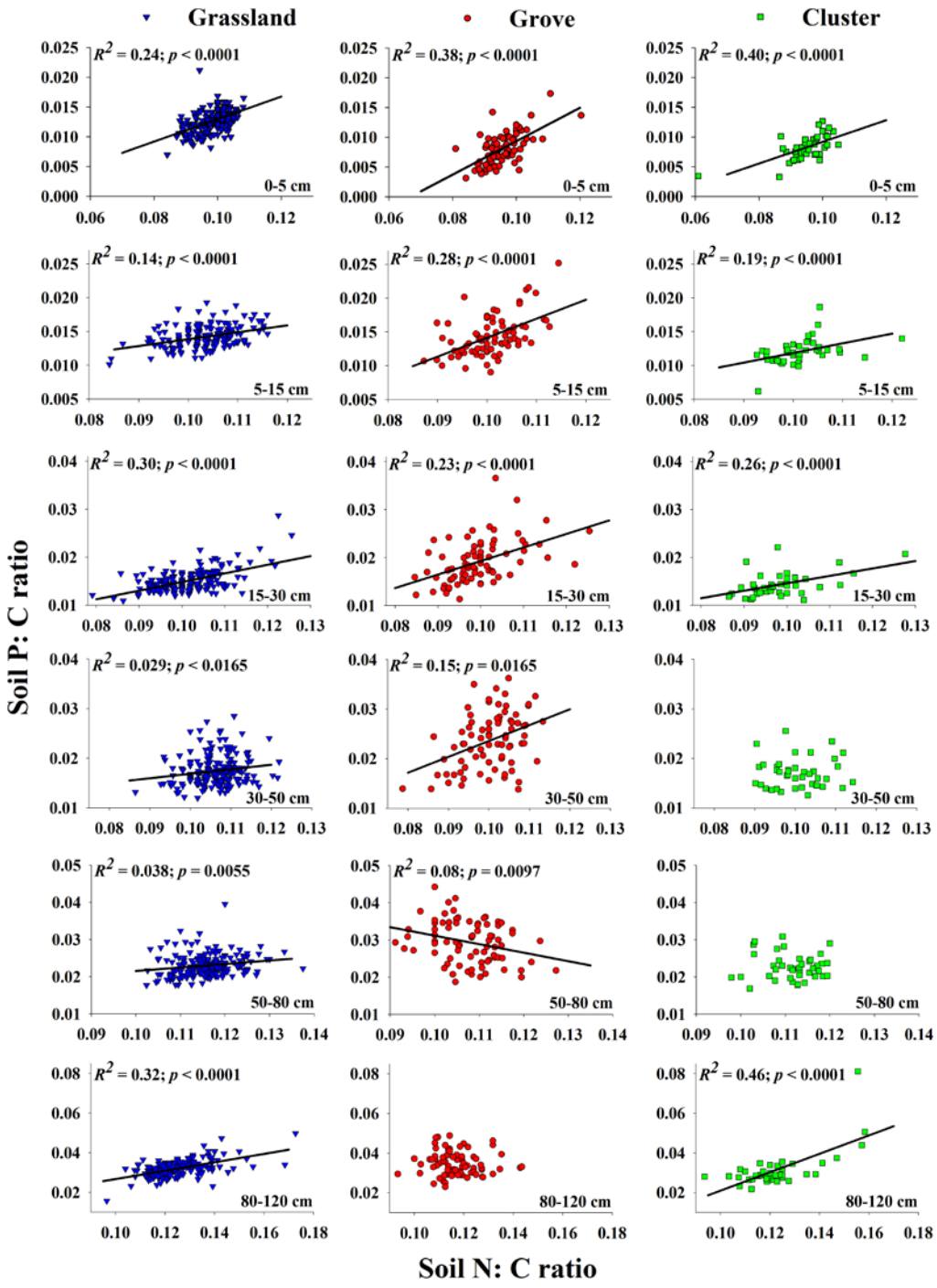

**Appendix S6**

Correlations between soil total phosphorus (mg P $kg^{-1}$ soil) and carbonate carbon (g C $kg^{-1}$ soil) through the soil profile. It should be noted that correlations in the surface soils (e.g. 0-5 cm and 5-15 cm) are probably driven more by the presence of snail shell fragments than by pedogenic carbonate formation. Snails were very evident across this landscape, especially beneath woody patches (personal observation). It should also be noted that < 10 % of the total 320 sampling points contained carbonate carbon in the surfaces soils (0-15 cm). Therefore, carbonate carbon in the surfaces soils (0-15 cm) were from snail shell particles that passed through 2 mm sieves.

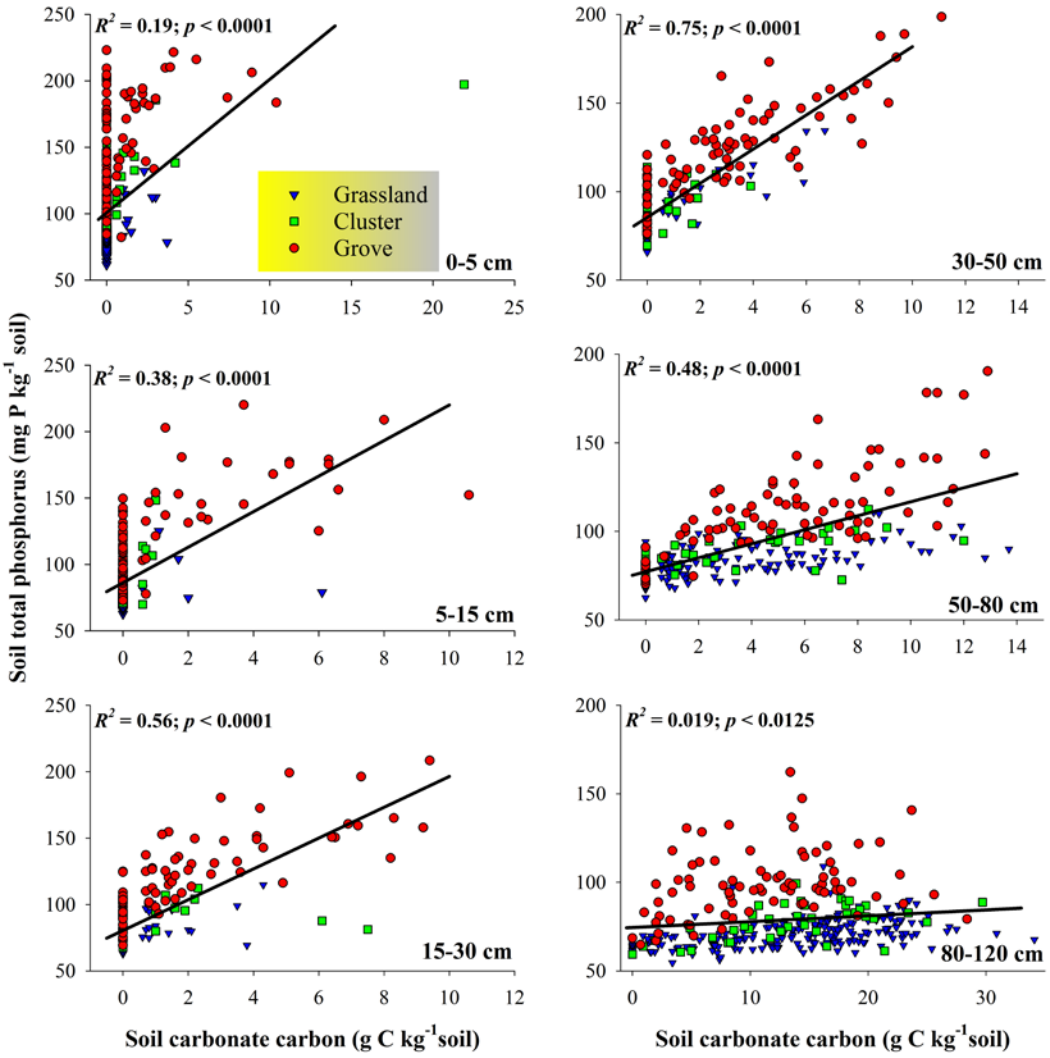

## Appendix S7

A *priori* structural equation model (a) showing influences of fine root density, soil clay and silt content, soil inorganic carbon, and soil pH on the accumulation of soil organic carbon (SOC), total nitrogen (TN) and total phosphorus (TP) in the 30-50 (b), 50-80 (c), and 80-120 (d) cm depth increments following woody plant encroachment. All variables are observed variables. Single-headed arrows point in the direction of causality, and double-headed arrows indicate correlations between variables. Numbers adjacent to arrows are standardized path coefficients. Continuous and dashed arrows represent positive and negative relationships, respectively, and arrow width is proportional to the magnitude of the standardized path coefficients. The proportion of variance explained ($R^2$) is shown alongside each response variable. Models for each soil depth were developed based on the combined data for grasslands, clusters, and groves (N = 320 samples/depth).

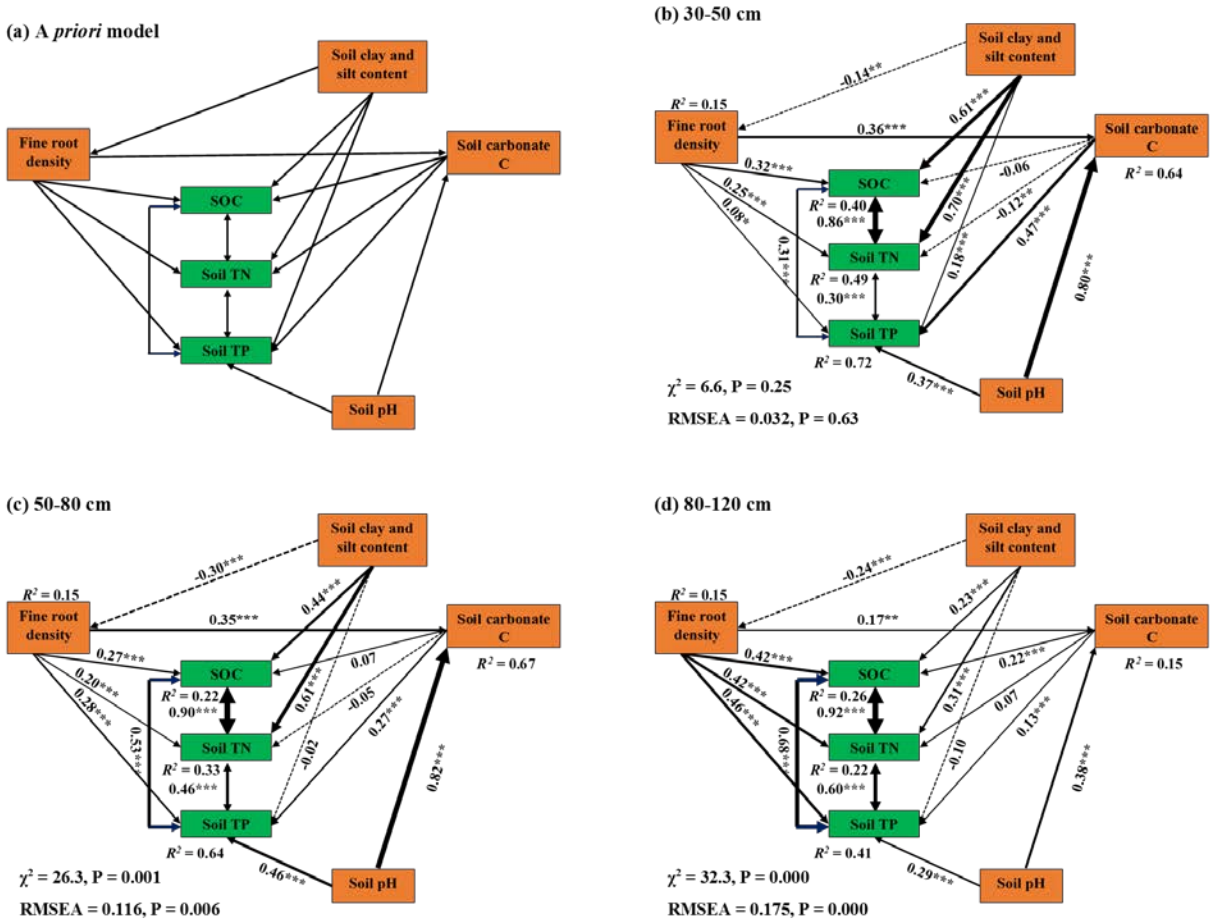

## References

McGroddy ME, Daufresne T, Hedin LO (2004) Scaling of C: N: P stoichiometry in forests worldwide: Implications of terrestrial Redfield-type ratios. *Ecology*, **85**, 2390-2401.

Zhou Y, Boutton TW, Wu XB (2017a) Woody plant encroachment amplifies spatial heterogeneity of soil phosphorus to considerable depth. *Ecology*, DOI: 10.1002/ecy.2051 (In press)